

AFRL-ML-WP-TP-2007-459

**NANOCOMPOSITES DERIVED FROM
A LOW-COLOR AROMATIC
POLYIMIDE (CP2) AND AMINE-
FUNCTIONALIZED VAPOR-GROWN
CARBON NANOFIBERS: IN SITU
POLYMERIZATION AND
CHARACTERIZATION (PREPRINT)**



**David H. Wang, Michael J. Arlen, Jong-Beom Baek, Richard A. Vaia,
and Loon-Seng Tan**

JANUARY 2007

Approved for public release; distribution unlimited.

STINFO COPY

**The U.S. Government is joint author of this work and has the right to use, modify,
reproduce, release, perform, display, or disclose the work.**

**MATERIALS AND MANUFACTURING DIRECTORATE
AIR FORCE RESEARCH LABORATORY
AIR FORCE MATERIEL COMMAND
WRIGHT-PATTERSON AIR FORCE BASE, OH 45433-7750**

NOTICE AND SIGNATURE PAGE

Using Government drawings, specifications, or other data included in this document for any purpose other than Government procurement does not in any way obligate the U.S. Government. The fact that the Government formulated or supplied the drawings, specifications, or other data does not license the holder or any other person or corporation; or convey any rights or permission to manufacture, use, or sell any patented invention that may relate to them.

This report was cleared for public release by the Air Force Research Laboratory Wright Site (AFRL/WS) Public Affairs Office and is available to the general public, including foreign nationals. Copies may be obtained from the Defense Technical Information Center (DTIC) (<http://www.dtic.mil>).

AFRL-ML-WP-TP-2007-459 HAS BEEN REVIEWED AND IS APPROVED FOR PUBLICATION IN ACCORDANCE WITH ASSIGNED DISTRIBUTION STATEMENT.

*//Signature//

LOON-SENG TAN, Research Group Leader
Polymer Branch
Nonmetallic Materials Division

//Signature//

JOHN F. MAGUIRE, Chief
Polymer Branch
Nonmetallic Materials Division

//Signature//

SHASHI K. SHARMA, Acting Deputy Chief
Nonmetallic Materials Division
Materials and Manufacturing Directorate

This report is published in the interest of scientific and technical information exchange, and its publication does not constitute the Government's approval or disapproval of its ideas or findings.

*Disseminated copies will show “//Signature//” stamped or typed above the signature blocks.

REPORT DOCUMENTATION PAGE				<i>Form Approved</i> OMB No. 0704-0188			
The public reporting burden for this collection of information is estimated to average 1 hour per response, including the time for reviewing instructions, searching existing data sources, gathering and maintaining the data needed, and completing and reviewing the collection of information. Send comments regarding this burden estimate or any other aspect of this collection of information, including suggestions for reducing this burden, to Department of Defense, Washington Headquarters Services, Directorate for Information Operations and Reports (0704-0188), 1215 Jefferson Davis Highway, Suite 1204, Arlington, VA 22202-4302. Respondents should be aware that notwithstanding any other provision of law, no person shall be subject to any penalty for failing to comply with a collection of information if it does not display a currently valid OMB control number. PLEASE DO NOT RETURN YOUR FORM TO THE ABOVE ADDRESS.							
1. REPORT DATE (DD-MM-YY) January 2007		2. REPORT TYPE Journal Article Preprint		3. DATES COVERED (From - To) N/A			
4. TITLE AND SUBTITLE NANOCOMPOSITES DERIVED FROM A LOW-COLOR AROMATIC POLYIMIDE (CP2) AND AMINE-FUNCTIONALIZED VAPOR-GROWN CARBON NANOFIBERS: IN SITU POLYMERIZATION AND CHARACTERIZATION (PREPRINT)				5a. CONTRACT NUMBER FA8650-05-D-5052			
				5b. GRANT NUMBER			
				5c. PROGRAM ELEMENT NUMBER 62102F			
6. AUTHOR(S) David H. Wang (University of Dayton Research Institute) Michael J. Arlen (University of Akron) Jong-Beom Baek (Chungbuk National University) Richard A. Vaia and Loon-Seng Tan (AFRL/MLBP)				5d. PROJECT NUMBER 4347			
				5e. TASK NUMBER RG			
				5f. WORK UNIT NUMBER M01R1000			
7. PERFORMING ORGANIZATION NAME(S) AND ADDRESS(ES) <table style="width: 100%; border: none;"> <tr> <td style="width: 30%; border: none; vertical-align: top;"> University of Dayton Research Institute 300 College Park Dayton, OH 45469-0168 ----- University of Akron Department of Polymer Science Akron, OH 44325 </td> <td style="border: none; vertical-align: top;"> Chungbuk National University Chungbuk 361-763 South Korea ----- Polymer Branch (AFRL/MLBP) Nonmetallic Materials Division Materials and Manufacturing Directorate Air Force Research Laboratory, Air Force Materiel Command Wright-Patterson Air Force Base, OH 45433-7750 </td> </tr> </table>				University of Dayton Research Institute 300 College Park Dayton, OH 45469-0168 ----- University of Akron Department of Polymer Science Akron, OH 44325	Chungbuk National University Chungbuk 361-763 South Korea ----- Polymer Branch (AFRL/MLBP) Nonmetallic Materials Division Materials and Manufacturing Directorate Air Force Research Laboratory, Air Force Materiel Command Wright-Patterson Air Force Base, OH 45433-7750	8. PERFORMING ORGANIZATION REPORT NUMBER	
				University of Dayton Research Institute 300 College Park Dayton, OH 45469-0168 ----- University of Akron Department of Polymer Science Akron, OH 44325	Chungbuk National University Chungbuk 361-763 South Korea ----- Polymer Branch (AFRL/MLBP) Nonmetallic Materials Division Materials and Manufacturing Directorate Air Force Research Laboratory, Air Force Materiel Command Wright-Patterson Air Force Base, OH 45433-7750		
9. SPONSORING/MONITORING AGENCY NAME(S) AND ADDRESS(ES) Materials and Manufacturing Directorate Air Force Research Laboratory Air Force Materiel Command Wright-Patterson AFB, OH 45433-7750				10. SPONSORING/MONITORING AGENCY ACRONYM(S) AFRL-ML-WP			
				11. SPONSORING/MONITORING AGENCY REPORT NUMBER(S) AFRL-ML-WP-TP-2007-459			
12. DISTRIBUTION/AVAILABILITY STATEMENT Approved for public release; distribution unlimited.							
13. SUPPLEMENTARY NOTES Journal article submitted to the Macromolecules. The U.S. Government is joint author of this work and has the right to use, modify, reproduce, release, perform, display, or disclose the work. PAO Case Number: AFRL/WS 07-0373, 20 Feb 2007. Paper contains color content.							
14. ABSTRACT Vapor-grown carbon nanofibers (VGCNF) were functionalized with amine-containing pendants via a Friedel-Crafts acylation reaction with 4-(3-aminophenoxy)benzoic acid. The resulting H2N-VGCNF with ca. 5 atom% functionalization was in attendance during the polymerization of 2,2-bis(phthalic anhydride)-1,1,1,3,3,3-hexafluoroisopropane (6FDA) and 1,3-bis(3-aminophenoxy)benzene (APB) in N,N-dimethylacetamide (DMAc) to afford a series of polyimide (CP2)-based nanocomposite films, which contained 0.1 to 5.0 wt% of H2N-VGCNF. For comparison purposes, the pristine VGCNF (0.1-5.0 wt%) was also used in the in situ polymerization of 6FDA and ABP. These two series of CP2/VGCNF nanocomposite films were cast from the respective polyamic acid/VGCNF DMAc solutions, followed by thermal imidization at curing temperatures up to 250 °C. The benefit and limitation of functionalized VGCNF on the length scale and the extent of CNF dispersion in a polyimide matrix were clear: (a) 0.1 wt% H2N-VGCNF film was visually transparent whereas similar (0.1 wt%) pristine VGCNF film showed the presence of large CNF aggregates throughout; (b) at 0.3 wt% H2N-VGCNF contents, the nanocomposite film had become translucent, and at 5 wt%, it was opaque. <i>(Continued on back of page)</i>							
15. SUBJECT TERMS Thermal and mechanical properties, CNT, carbon fiber reinforced epoxy							
16. SECURITY CLASSIFICATION OF:			17. LIMITATION OF ABSTRACT: SAR	18. NUMBER OF PAGES 58	19a. NAME OF RESPONSIBLE PERSON (Monitor) Loon-Seng Tan 19b. TELEPHONE NUMBER (Include Area Code) N/A		
a. REPORT Unclassified	b. ABSTRACT Unclassified	c. THIS PAGE Unclassified					

14. ABSTRACT (concluded)

Since CP2 is very soluble in THF, the CP2-grafted VGCNF were simply separated from the free CP2 by solvent extraction. The molecular weights of the extracted CP2 were measured using gel-permeation chromatography (GPC). The effects of VGCNF on molecular weight (MW) and glass-transition (T_g) were discussed in terms of GPC and thermal analysis results, respectively. The dispersion of VGCNF in CP2 was evaluated using scanning electron microscopy (SEM). The tensile properties of the nanocomposite films were determined, showing up to 45% increase in modulus as the functionalized VGCNF content raised to 5 wt%.

**NANOCOMPOSITES DERIVED FROM A LOW-COLOR AROMATIC POLYIMIDE
(CP2) AND AMINE-FUNCTIONALIZED VAPOR-GROWN CARBON NANOFIBERS:
IN SITU POLYMERIZATION AND CHARACTERIZATION**

David H. Wang ^a, Michael J. Arlen ^b, Jong-Beom Baek ^c,

Richard A. Vaia ^d, and Loon-Seng Tan ^{d*}

^a University of Dayton Research Institute, Dayton Ohio 45469-0168 USA

^b Department of Polymer Science, University of Akron, Akron, Ohio 44325

^c Department of Industrial Chemistry, Chungbuk National University, Chungbuk, 361-763,
South Korea

^d Polymer Branch, AFRL/MLBP, Materials & Manufacturing Directorate, Air Force Research
Laboratory, Wright-Patterson AFB, OH 45433-7750 USA

* Correspondence to: Loon-Seng Tan, (937)255-9141; Fax (937)255-9157

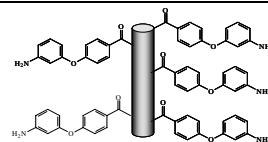
Email: loon-seng.tan@wpafb.af.mil

TOC Summary and Graphic

David H. Wang, Michael J. Arlen, Jong-Beom Baek, Richard A. Vaia, and Loon-Seng Tan*

In situ nanocomposite films derived from a low-color aromatic polyimide (CP2) and amine-functionalized vapor-grown carbon nanofibers

Vapor-grown carbon nanofibers (VGCNF) were functionalized with amine-containing pendants via a Friedel-Crafts acylation reaction with 4-(3-aminophenoxy)benzoic acid. The resulting H₂N-VGCNF with ca. 5 atom% functionalization was used to generate a series of polyimide(CP2)-based in situ nanocomposite films that contained 0.1 to 5.0 wt% of H₂N-VGCNF and showed improved dispersion and tensile modulus.



0.1 wt% NH₂-VGCNF

0.1 wt% Pristine VGCNF

Abstract:

Vapor-grown carbon nanofibers (VGCNF) were functionalized with amine-containing pendants via a Friedel-Crafts acylation reaction with 4-(3-aminophenoxy)benzoic acid. The resulting H₂N-VGCNF with ca. 5 atom% functionalization was in attendance during the polymerization of 2,2-bis(phthalic anhydride)-1,1,1,3,3,3-hexafluoroisopropane (6FDA) and 1,3-bis(3-aminophenoxy)benzene (APB) in N,N-dimethylacetamide (DMAc) to afford a series of polyimide(CP2)-based nanocomposite films, which contained 0.1 to 5.0 wt% of H₂N-VGCNF. For comparison purposes, the pristine VGCNF (0.1-5.0 wt%) was also used in the in situ polymerization of 6FDA and ABP. These two series of CP2/VGCNF nanocomposite films were cast from the respective polyamic acid/VGCNF DMAc solutions, followed by thermal imidization at curing temperatures up to 250 °C. The benefit and limitation of functionalized VGCNF on the length scale and the extent of CNF dispersion in a polyimide matrix were clear: (a) 0.1 wt% H₂N-VGCNF film was visually transparent whereas similar (0.1 wt%) pristine VGCNF film showed the presence of large CNF aggregates throughout; (b) at 0.3 wt% H₂N-VGCNF contents, the nanocomposite film had become translucent, and at 5 wt%, it was opaque. Since CP2 is very soluble in THF, the CP2-grafted VGCNF were simply separated from the free CP2 by solvent extraction. The molecular weights of the extracted CP2 were measured using gel-permeation chromatography (GPC). The effects of VGCNF on molecular weight (MW) and glass-transition (T_g) were discussed in terms of GPC and thermal analysis results, respectively. The dispersion of VGCNF in CP2 was evaluated using scanning electron microscopy (SEM). The tensile properties of the nanocomposite films were determined, showing up to 45% increase in modulus as the functionalized VGCNF content raised to 5wt%.

Introduction

One-dimensional, carbon-based nanomaterials can be broadly classified according to their diameter dimensions as follows: (i) single-wall carbon nanotube or SWNT (0.7-3 nm); (ii) multi-wall carbon nanotube or MWNT (2-20 nm); (iii) carbon nanofiber or CNF (40-100 nm).¹ Since the hollow structure of CNF is also made up of concentric graphitic layers, some researchers have considered it to be MWNT when its average diameter is less than 100 nm. In comparison to SWNT or MWNT, CNF is more attractive for its relatively low cost and availability in larger quantities as the result of their more advanced stage in commercial production. However, while there is a more wide-spread interest on the functionalization chemistry of SWNT and MWNT in the materials research community with the common objective of improving their dispersibility/solubility in organic solvents or aqueous media and optimizing the nanoscale dispersion and interfacial adhesion in solid matrices.^{2,3,4,5} There are only relatively few reports on the chemical modification of CNF.^{6,7}

Recently, we have developed an effective method to directly arylcarbonylate vapor-grown carbon nanofibers (VGCNF) via Friedel-Crafts (F-C) acylation reaction in poly(phosphoric acid) (PPA) with aromatic carboxylic acids, and also applied the technique to graft a linear poly(ether-ketone) or a hyperbranched poly(ether-ketone) onto pristine CNF/carbon nanotube (CNT) to generate the so-called in situ nanocomposites in a one-pot fashion.⁶ Subsequently, in addition to extending the applicability of this functionalization method to MWNT, we have found useful functionalities such as OH and NH₂ to be chemically unaffected in the PPA-promoted F-C acylation. The VGCNF or MWNT pre-functionalized with these reactive groups would permit investigation into their effects on the in situ polymerization process and the resulting nanocomposites prepared in a two-stage fashion. Specifically, NH₂-functionalized CNF/CNT would be valuable in the preparation of polyimide-based nanocomposites. Polyimides display a unique combination of excellent mechanical, electrical and optical properties and outstanding thermal stability. Their monomers are readily available or relatively easy to prepare compared to those of other high performance polymers. Thus, polyimides have found many applications in high performance films and fibers, coatings, microelectronics, optoelectronics, adhesives, aerospace, nonlinear-optical devices, light-wave guide materials, and liquid crystal displays.⁸ The polyimide known as CP2 that is derived from 2,2-bis(phthalic anhydride)-1,1,1,3,3,3-hexafluoroisopropane (6FDA) and 1,3-bis(3-

aminophenoxy)benzene (APB) was selected for this work, primarily because of extensive preparation and characterization studies have been conducted on the nanocomposites of this polyimide and CNF/CNT. Thus, the pertinent synthesis, dispersion and property data are available for comparison.⁹

Experimental

Materials. Vapor grown carbon nanofiber (VGCNF, PR-19-HT) was obtained from Applied Science Inc., Cendarville, OH. VGCNF are produced by a vapor-phase catalytic process in which a carbon-containing feedstock (e.g., CH₄, C₂H₄, etc.) is pyrolyzed in the presence of small metal catalyst (e.g., ferrocene, Fe(CO)₅, etc.). They have an outer diameter of 60-200 nm, a hollow core of 30-90 nm, and length on the order of 50-100 μ m.^{1,10,11} All other chemicals were reagent-grade and purchased from Aldrich Chemical Inc. and used as received, unless otherwise specified. N-Methyl-2-pyrrolidinone (NMP) was distilled under reduced pressure over phosphorous pentoxide. Anhydrous DMAc and other solvents were used as received. 2,2-bis(phthalic anhydride)-1,1,1,3,3,3-hexafluoroisopropane (6FDA; $\geq 99\%$) was purchased from Aldrich and used as received. 1,3-bis(3-aminophenoxy)benzene (ABP) was (99% min.) was purchased from Chriskev Company, Inc.¹² and used as received.

Instrumentation. Proton and carbon nuclear magnetic resonance (¹H-NMR and ¹³C-NMR) spectra for intermediates, monomer, and polymers were measured at 500 MHz on a Tecmag-500 spectrometer. Infrared (IR) spectra were recorded on a Nicolet Nexus 470 Fourier transform spectrophotometer. Elemental analysis and mass spectral analysis were performed by System Support Branch, Materials Directorate, Air Force Research Lab, Dayton, Ohio. The melting points (m.p.) of all compounds were determined on a Mel-Temp melting point apparatus and are uncorrected. Intrinsic viscosities were determined with Cannon-Ubbelohde No. 75 viscometer. Flow times were recorded in NMP solution and polymer concentrations were approximately 0.5-0.10 g/dL at 30.0 \pm 0.1°C. Lithium bromide (1.0wt%) was added to the solution to eliminate polyelectrolyte effect. Differential scanning calorimetry (DSC) analysis were performed in nitrogen with a heating rate of 10°C/min using a Perkin-Elmer model 2000 thermal analyzer equipped with differential scanning calorimetry cell. Thermogravimetric analysis (TGA) was conducted in nitrogen (N₂) and air atmospheres at a heating rate of 10°C/min using a TA Hi-Res TGA 2950 thermogravimetric analyzer. Gel permeation

chromatography (GPC) was carried out on an Agilent 1100 Series equipped with refractive index and light scattering detectors. Tetrahydrofuran (THF) was used as the eluting solvent. The scanning electron microscope (SEM) used in this work was a Hitachi S-5200. Wide-angle X-ray diffractions (WAXS) of compression-molded samples were recorded with a Rigaku RU-200 diffractometer using Ni-filtered Cu KR radiation (40 kV, 100 mA, $\lambda=0.15418$ nm). Tensile strength and moduli of the polyimide films were tested using Tinius Olsen H10K-S Benchtop Testing Machine with a crosshead separation speed of 1 mm/min. Sonication was conducted at 20 kHz with a 600W-power using Ace Glass GEX 600-5 Ultrasonic Processor.

4-(3-Aminophenoxy)benzonitrile (3)¹³: Into a 250 ml three-necked flask equipped with a magnetic stirrer, a Dean-Stark trap, a nitrogen inlet and outlet, 4-nitrobenzonitrile (7.41 g, 50.0 mmol), 3-aminophenol (5.46 g, 50 mmol), potassium carbonate (8.28 g, 60.0 mmol), NMP (100 mL) and toluene (50 mL) were charged and stirred with dried nitrogen purging at 160 °C for 6 h. The mixture was allowed to cool to room temperature and filtered. The filtrate was poured into water. The white solid was collected by filtration and dried. It was dissolved in acetone and precipitated into water to afford 8.18 g (78% yield) of white solid, m.p. 88-90 °C (Lit.^{12a} 84-88 °C). Anal. Calcd. for C₁₃H₁₀N₂O: C, 74.27%; H, 4.79%; N, 13.32%. Found: C, 74.09%; H, 4.86%; N, 13.35%. FT-IR (KBr, cm⁻¹): 3486, 3392 (NH₂), 2218 (nitrile), 1629 (carbonyl). Mass spectrum (m/e): 210 (M⁺). ¹H-NMR (DMSO-d₆, δ in ppm): 5.38 (s, 2H, NH₂), 6.22-6.25 (dd, 1H, Ar-**H**), 6.30-6.32 (t, 1H, Ar-**H**), 6.46-6.50 (dd, 1H, Ar-**H**), 7.06-7.12 (m, 3H, Ar-**H**) and 7.80-7.83 (d, 2H, Ar-**H**). ¹³C-NMR (DMSO-d₆, δ in ppm): 104.59, 105.05, 106.90, 110.83, 117.91, 118.86, 130.48, 134.48, 150.89, 155.37, 161.44.

4-(3-Aminophenoxy)benzoic acid (4)¹⁴: Into a 100 ml three-necked flask equipped with a magnetic stirrer, a nitrogen inlet and outlet, 4-(3-aminophenoxy)benzonitrile (5.00 g, 24.0 mmol), polyphosphoric acid (83% P₂O₅ assay, 30.0 g) and water (5.30 g, 60.0 mmol) were charged and stirred with dried nitrogen purging at 120 °C for 8 h. The mixture was poured into water and the yellow solid was collected by filtration. It was recrystallized in water/ethanol (50:50) mixture to afford 4.50 g (83% yield) of yellow crystals, m.p. 145-147 °C (Lit.¹³ 145-147 °C). Anal. Calcd. for C₁₃H₁₀N₂O: C, 68.11%; H, 4.84%; N, 6.11%. Found: C, 68.36%; H, 4.90%; N, 6.23%. FT-IR (KBr, cm⁻¹): 3446, 3356 (NH₂), 2500-3500 (broad, COOH), 3212, 3071, 1657 (carbonyl), 1600, 1485, 1393, 1237, 1174, 853, 772. Mass spectrum (m/e): 229 (M⁺). ¹H-NMR (DMSO-d₆, δ in ppm): 6.21-6.24 (dd, 1H, Ar-**H**), 6.27-6.28 (t, 1H, Ar-**H**), 6.41-

6.45 (dd, 1H, Ar-**H**), 6.99-7.09 (m, 3H, Ar-**H**) and 7.92-7.95 (d, 2H, Ar-**H**). ^{13}C -NMR (DMSO- d_6 , δ in ppm): 104.81, 106.74, 110.32, 117.14, 124.68, 130.23, 131.44, 150.47, 155.74, 161.18, 166.71.

Functionalization of VGCNF with 3-aminophenoxy-4-benzoic acid (6, H₂N-VGCNF): Into a 250 mL resin flask equipped with a high torque mechanical stirrer, and nitrogen inlet and outlet, 3-aminophenoxy-4-benzoic acid (0.50 g, 2.18 mmol) and VGCNF (0.50 g), PPA (83% P₂O₅ assay, 20 g) and phosphorus pentoxide (P₂O₅, 5.0 g) were charged and stirred with dried nitrogen purging at 130 °C for 72 h. After cooling down to room temperature water was added. The resulting precipitate was collected, washed with diluted ammonium hydroxide and Soxhlet extracted with water for three days and methanol for three days. It was then dried over P₂O₅ under reduced pressure at 72 h for 72 h to afford 0.80 g (83% yield) of dark brown solid. Anal. Calcd. For C₁₆₅H₅₀N₅O₁₀ (based on the assumption that for every 100 carbon, there are 5 3-aminophenoxy-4-benzoyl groups attached): C, 87.60%; H, 2.11%; N, 3.10%; O, 7.07%. Found: C, 87.11%; H, 2.33%; N, 3.43%; O, 6.40%. FT-IR (KBr, cm⁻¹): 3441, 3008, 1624 (carbonyl), 1597, 1486, 1227, 1170.

PPA-treated VGCNF (7, PT-VGCNF): Compound **7** was synthesized from VGCNF (0.50 g), PPA (83% P₂O₅ assay, 20 g) and phosphorus pentoxide (P₂O₅, 5.0 g) using the same procedure used for compound **6** to afford 0.47 (94% yield) of a black solid. Anal. Found: C, 98.66%; H, 0.93%; N, <0.20%; O, <0.10%.

Representative procedure for in situ polymerization (CP2 with 1.0 wt% VGCNF load). Into a 50 mL three necked flask equipped with a magnetic stirrer, nitrogen inlet and outlet, H₂N-VGCNF (**3**, 45.0 mg) and anhydrous DMAc (20 mL) were placed and sonicated for 30 min until the H₂N-VGCNF was dispersed in NMP homogeneously. 6FDA (1.777 g, 4.0 mmol) was added and stirred under dry nitrogen at room temperature for 30 min. Then APB (1.158 g, 3.96 mmol) was charged. The dark mixture was agitated at room temperature for 24 h to afford a viscous poly(amic acid) (PAA). The resulting mixture was diluted with DMAc (20 mL), poured into a glass dish, followed by vacuum evaporation of DMAc and heat-treatment at 100 °C/24h; 150 °C/4h; 200 °C/2h and 250 °C/1h. The film thickness is about 0.1 mm. FT-IR (KBr, cm⁻¹): 3442, 3087, 1785, 1718 (imide), 1587, 1477, 1365, 1429, 1187, 1096, 962, 855.

Results and Discussion

Synthesis and Characterization of H₂N-VGCNF. The diameter and length of the VGCNF (Pyrograf III-19-HT) used in this work were in the ranges 50-100 nm and 5-30 μ m, respectively. It follows that having aspect ratios (length/diameter) of in the range of 100-600 should make them useful as nanolevel reinforcement for polymeric matrices. Furthermore, since their inherent electrical and thermal transport properties are also excellent, there are many possibilities imaginable for tailoring their polymer matrix composites into affordable, lightweight, multifunctional materials.

These VGCNF were heat-treated up to 3000 °C to graphitize the surface carbon and remove residual iron catalyst and to improve the associated conducting properties. The as-received VGCNF contains 1.01 wt % of hydrogen determined by elemental analysis (Table 1), presumably attributable to the sp³ C-H and sp² C-H defects as methane is used as the major component in the feedstock for its production. Based on hydrogen content, there is approximately 11.5 atom% of C-H defects in VGCNF. These defects would provide sites susceptible to the electrophilic substitution (Friedel-Crafts acylation) reaction.⁶

[Table 1. Element analysis data for pristine NH₂-VGCNF and PT-VGCNF]

The amine-containing acylating agent, namely, 3-aminophenoxy-4-benzoic acid (**4**) was prepared using a two-step synthetic route (Scheme 1). The nucleophilic nitro-displacement of 4-nitrobenzonitrile (**2**) with 3-aminophenol (**1**) in the presence of potassium carbonate yielded 3-aminophenoxy-4-benzonitrile (**3**), which was subsequently hydrolyzed in 100% of phosphoric acid to afford 3-aminophenoxy-4-benzoic acid (**4**).

[Scheme 1. Functionalization of VGCNF with 3-aminophenoxy-4-benzoic acid (i) NMP, K₂CO₃, 160 °C, 6 h. (ii) PPA, H₂O, 120 °C, 8 h. (iii) P₂O₅/PPA, 130 °C, 3 d.]

Based on the results of our previous work on the model-compound and related in situ polymerization studies, we have reported that Friedel-Crafts (F-C) acylation in poly(phosphoric acid) (PPA) is a viable, alternative route to effecting a controlled functionalization of VGCNF and MWNT.⁶ Thus, VGCNF and MWNT were not only functionalized with the aid of 2,4,6-trimethylphenoxybenzoic acid as a model compound to probe, validate and quantify the extent of

surface modification, but also were grafted with meta-poly(ether-ketone) (*m*PEK) and hyperbranched PEK via in situ polymerization with appropriate AB and AB2 monomers using optimized PPA conditions that we previously described.¹⁵ On account of significant hydrogen content analyzed in the starting VGCNF and MWNT, it was concluded that the covalent attachment of the arylcarbonyl groups most probably occurred at the sp^2C-H sites.

Amine functionality is one of the most versatile groups in polymer chemistry and various efforts reported to modify carbon nanosurfaces with amino groups.¹⁶ In order to functionalize VGCNF with an amine group, we rationalized that amine group should be deactivated upon protonation in PPA and would not interfere with the intended F-C acylation reaction. Thus, we selected compound **4** (aminophenoxy-4-benzoic acid)¹³ a simple acylating agent containing both carboxylic acid and amine groups. Subsequently, VGCNF was treated with **4** at 130 °C in PPA/P₂O₅ via F-C acylation to afford an amine-functionalized VGCNF (NH₂-VGCNF, **6**) as shown in Scheme 1. Compound **4** exhibits carboxylic carbonyl stretches at 1657 cm⁻¹ and a broad band at 2500-3500 cm⁻¹. The vibration bands of primary amine appear at 3446 (asym.) and 3356 (sym.) cm⁻¹. After F-C reaction, the carbonyl absorption of compound **6** is shifted to 1624 cm⁻¹ as expected. The broad band at 2500-3500 cm⁻¹, which is associated with the hydroxyl stretch of carboxylic acid, has disappeared. The amine absorption becomes weak “spikes” at 3441 and 3384 cm⁻¹, sitting on top of the broad band attributable to the absorbed water in the KBr (Figure 1). These observed changes in the IR spectra indicate a successful grafting reaction. Furthermore, the scanning electron microscopy (SEM) revealed that the pristine VGCNF exhibits smooth textures on the surface whereas the rough surfaces of the functionalized VGCNF are clearly indicative of modification with organic moieties (Figure 2).

[Figure 1. FT-IR spectra of (a) pristine VGCNF, (b) PT-VGCNF, (c) 3-aminophenoxy-4-benzoic acid (**4**) and (d) NH₂-VGCNF (**6**).]

[Figure 2. SEM images of (a) as-received VGCNF (×100k) and (b) NH₂-VGCNF (×70k).]

The pristine VGCNF shows excellent thermal stability in both air and helium as shown in Figure 3. In air, the unmodified VGCNF underwent a catastrophic weight loss at temperatures >700 °C and fairly stable up to 900 °C in helium. In the case of **6**, we expected that the onset of

weight loss under either air or helium atmosphere should commence at much lower temperatures because of the organic pendants. Indeed, NH_2 -VGCNF started to lose weight at 247 in air and 243 °C in helium, respectively, due to the decomposition of organic amine groups. The TGA curve taken in air showed a two-stage degradation. NH_2 -VGCNF lost 45.6% of weight between 250 and 700 °C, attributable to the loss of arylcarbonyl substituents, with 55.4% of residue at 700 °C due to VGCNF. It is important to point out that the subsequent degradation pattern of **6** is practically congruent with that of the unmodified VGCNF in the 700–900 °C region. Based on TGA and element analysis results (Table 1 and Figure 3), we concluded that there were approximately 5 arylcarbonyl groups covalently attached to the nanofiber surface for every 100 carbon sites.

[Figure 3. TGA thermograms with heating rate of 10 °C/min of pristine VGCNF and H_2N -VGCNF]

PPA-treated VGCNF. In order to investigate the effect of PPA/ P_2O_5 on VGCNF, a control experiment was run where VGCNF without TMPBA was heated in PPA/ P_2O_5 at 130 °C for three days to afford a PPA-treated VGCNF (PT-VGCNF) in 94% yield as shown in Scheme 2. The work-up was the same as that for NH_2 -VGCNF. The IR spectrum of PT-VGCNF is essentially the same as that of the pristine VGCNF (see Fig. 1). PT-VGCNF has slightly lower carbon and hydrogen contents than pristine VGCNF, although the differences are in the range of testing errors (Table 1). In addition, the pristine and PT-VGCNF share the same morphologies including surface, diameter and length (Figure 4). All these results point out that PPA is a mild, non-destructive medium for F-C reactions on carbon nanosurfaces.

[Scheme 2. PPA-treated VGCNF (i) P_2O_5 /PPA, 130 °C, 3 d.]

[Figure 4. SEM images of (a) as-received VGCNF ($\times 25\text{k}$) and (b) PT-VGCNF ($\times 25\text{k}$).]

***In situ* Polymerization and Characterization of Polyimide-CP2 in presence of H_2N -VGCNF.** The polymerization of the dianhydride 6FDA (**8**) and the diamine APB (**9**) was conducted in the presence of well-dispersed H_2N -VGCNF (**6**) in DMAc at room temperature for

24 h to afford poly(amic acid)-g-VGCNF solutions (**10**). The resulting viscous and yellow solutions were diluted with DMAc and then poured into a glass dish, followed by curing at an elevated temperature to afford a series of CP2-g-VGCNF films (**11**) as shown in Scheme 3. The functionalized-VGCNF content in these films was set at 0, 0.1, 0.3, 1.0, 2.0 and 5.0 wt%. In a set of comparison experiments, the pristine VGCNF was used during the in situ polymerization of 6FDA (**8**) and APB (**9**) to afford PAA solutions (**12**), followed by the same curing protocol as CP2-g-VGCNF to afford another series of CP2/VGCNF films (**13**) as shown in Scheme 4. The pristine-VGCNF contents were also 0.1, 0.3, 1.0, 2.0 and 5.0 wt%.

[Scheme 3. Synthesis of CP2-g-VGCNF nanocomposites via in situ polymerization of 6FDA (**7**), APB (**8**) and H₂N-VGCNF (**6**): (i) DMAc, room temperature; (ii) 100 °C, 24h; 150 °C, 4h; 200 °C, 2h; 250 °C, 1h.]

[Scheme 4. Synthesis of VGCNF/CP2 blends via in situ polymerization of 6FDA (**7**), APB (**8**) and pristine VGCNF (**5**). (i). DMAc, room temperature, 24h. (ii). 100 °C, 24h; 150 °C, 4h; 200 °C, 2h; 250 °C, 1h.]

The neat CP2 film is slightly yellow as shown in Figure 5. The dispersion of H₂N-VGCNF (0.1 wt%) in the CP2-g-VGCNF film is more uniform than the corresponding 0.1 wt% of the pristine VGCNF in the CP2/VGCNF film, which contains large aggregated clusters of VGCNF. The polymer film containing 0.3 wt% of H₂N-VGCNF is still translucent while the films containing more than 1.0 wt% of H₂N-VGCNF have become opaque.

[Figure 5. CP2 films containing VGCNF]

Solution Properties. In order to investigate the effect of VGCNF on molecular weights (MWs) of CP2, both CP2-g-VGCNF and CP2/VGCNF films were weighed and added to THF for two days. Then, the mixtures were filtered through a 0.8 µm PTFE membrane and washed with large amount of THF. The filtrates containing soluble polyimides (THF-soluble CP2) were concentrated and the MWs were determined by gel-permeation chromatography (GPC) using polystyrene standards. The residual black solids or films were collected, dried and weighed to

determine an “insoluble content in THF” as shown in Tables 2 and 3. It is reasonable to assume that the THF-insoluble fractions comprise the polymer-grafted VGCNF because the amounts are much larger than the respective VGCNF feed amounts and they were soluble in amide solvents and methanesulfonic acid (*infra vida*). The molecular weights of the polyimide grafts on VGCNF were calculated based on the assumption that there were 5 arylcarbonylation sites for every 100 carbons of the VGCNF (Table 1). The number average (M_n) and weight average (M_w) MWs of the neat CP2 are 84,200 and 238,400 Da., respectively. For CP2-g-VGCNF the M_n s of THF-soluble CP2 increase to 126,300 with 0.1 wt% of VGCNF and then decrease gradually 41,900 Da. as VGCNF contents increase to 5.0 wt%. The MW of grafted CP2 is 5,280 Da. for 0.1 wt% CP2-g-VGCNF film and decrease to 2,280 Da. for 5wt% film according to the calculation explained in Table 2. The decrease of molecular weights is due to the increase of amine groups as the NH_2 -VGCNF contents increase.

For CP2/VGCNF (blend) films, although the M_n of THF-soluble CP2 increase to 126,200 with 0.1 wt% of VGCNF, the M_n values decrease gradually to 57,090 Da. as VGCNF contents increase to 5.0 wt%. The insoluble contents in THF for CP2/VGCNF are similar to the VGCNF contents, providing the evidence that there are practically no physically adsorbed CP2 in these blends (Table 3).

It seems that at the low concentration (0.1 wt%), both pristine and functionalized VGCNFs increase the molecular weights of CP2. The viscosities of polyamic acids have been observed to decrease over days after preparation.¹⁷ The initial high molecular weights were resulted from the interfacial polymerization between diamines and dianhydrides. Polyamic acids re-equilibrated to lower molecular weights. It is possible that VGCNF promotes the interfacial polymerization at lower concentration during the preparation of polyamic acids or slow down the re-equilibration, resulting in higher CP2 molecular weights. On the other hand, the decrease of molecular weight at higher VGCNF concentrations could be attributed to decreased mobility of the aromatic diamine, resulting from π - π overlap interactions with VGCNF surface.¹⁸ For CP2-g-VGCNF, NH_2 -VGCNF could serve as an end capping agent during the in situ polymerization and cause the stoichiometric imbalance between diamine and dianhydride, leading to lower MWs. Nevertheless, the molecular weights of all the CP2 polymers extracted into THF are higher than 40,000 Da., which are assumed to be high enough for the overall properties of the polyimides to be unaffected.

[Table 2. Molecular weights and MW distributions of CP2-g-VGCNF nanocomposite films]

[Table 3. Molecular weights and MW distributions of CP2/VGCNF blend films]

Interestingly, the nanocomposite film containing 5 wt% CP2-g-VGCNF was swollen with little loss in its structural integrity after a two-day extraction in THF, whereas the similar CP2/VGCNF film disintegrated into powders due to the dissolution of CP2-polyimide in THF (Figures 6 and 7). At first we suspected that CP2 formed cross-linked networks with NH₂-VGCNF and became solvent-resistant. However, we found that these nanocomposite films were soluble in stronger solvents such as DMAc, NMP and methanesulfonic acid. In fact, the intrinsic viscosities of CP2-g-VGCNF nanocomposites were measured in NMP (Table 4). The viscosity of pristine CP2 is 0.42 dL/g while the viscosities of the nanocomposites increase from 0.65 to 1.43 dL/g as the VGCNF contents increase from 0.1 to 5 wt%. Although the molecular weights of CP2-g-VGCNF decrease with the VGCNF contents, their viscosities increase due to the large aspect ratios of VGCNF.

[Figure 6. CP2 film during THF extraction (a) 5wt% CP2-g-VGCNF and (b) 5wt% CP2/VGCNF blend.]

[Figure 7. CP2 film after THF extraction (a) 5wt% CP2-g-VGCNF and (b) 5wt% CP2/VGCNF (physical blend).]

Thermal Properties. The glass-transition (T_g) temperatures of CP2-g-VGCNF and CP2/VGCNF samples were determined by DSC. The powder samples were heated to 300 °C in the DSC chamber in the first run and cooled to ambient temperature at 10 °C/min under nitrogen purge. Then the samples were heated to 300 °C at 10 °C/min in the second run. The T_g 's were calculated based on mid-point of change in slope on the second heating run. In previous work, we observed the T_g 's of *m*-polyetherketone (*m*PEK) increased gradually with VGCNF contents after *m*PEK was grafted onto VGCNF.^{6(b)} This is consistent with the rationale that the attachment of flexible *m*PEK chains to the rigid VGCNF surface imposes constraints over their mobility,

resulting in increase in the glass-transition temperature. However, we observed some unusual thermal behaviors for both CP2-g-VGCNF and CP2/VGCNF films. The glass transition temperature of CP2-polyimide is 199 °C. The T_g values of 0.1 wt % and 0.3 wt% CP2-g-VGCNF films increase to 201 °C and 202 °C, respectively. As the VGCNF contents were incrementally increased from 0.3 wt% to 5wt%, the T_g 's of CP2-g-VGCNF films decrease from 201 to 196 °C (Table 2 and Figure 8a). The T_g 's of CP2/VGCNF films change similarly to those of CP2-g-VGCNF films. The T_g of 0.1 wt % CP2/VGCNF film increased from 199 °C (CP2) to 203 °C. Then the T_g 's decreased to 202 °C for 0.3 wt% CP2/VGCNF film, and further decreased to 194 °C as VGCNF contents increase to 5 wt% (Table 3 and Figure 8b). Since the M_n values of CP-g-VGCNF and CP2/VGCNF films are relatively high (>40,000 Daltons), it was unexpected that the T_g 's decreased with VGCNF contents, too. A possible explanation invokes presence of the micro-voids formed between CP2 and VGCNF due to CP2 shrinkage during the thermal imidization process. The micro-voids act collectively as free volume in polymer matrix. As the free volume of a polymer increases, its T_g decreases.¹⁹ Thus, as the numbers of the micro-voids (the overall size of free volume) increased with VGCNF contents, the glass transition of the CP2 polymer in the nanocomposites and physical blends was depressed accordingly. Waltson et al also observed T_g decreases with addition of CNTs and VGCNF into polyimides.²⁰ Similar results have been observed when nanoclay and bentonite were blended with epoxies and cyanate ester, respectively,²¹ where the free volume fractions increased with the contents of nanoclay and bentonite. The T_g 's of the resulting nanocomposites decreased accordingly in most occasions.

Thermogravimetry analysis (TGA) results showed that all the film samples exhibited excellent thermal and thermo-oxidative stabilities, with 5% weight loss temperature ranging from 524-531 °C in helium and 518-526 °C in air, respectively (Figure 9, Tables 4 and 5).

[Figure 8. DSC thermograms of (a) CP2-g-VGCNF samples and (b) CP2/VGCNF blends with heating rate of 10 °C/min]

[Table 4. Physical properties of CP2-g-VGCNF films]

[Table 5. Thermal properties of CP2/VGCNF films]

[Figure 9. TGA thermograms of CP2-g-VGCNF with heating rate of 10 °C/min (a) in air and (b) in helium]

Infra-red Spectra. The films of CP2-polyimide, 5 wt% CP2-g-VGCNF, and 5 wt% CP2/VGCNF were subjected to attenuated total reflectance Fourier-transform infrared (ATR-FTIR) measurements. CP2 shows a strong absorption band at 1718 cm^{-1} and weak one at 1778 cm^{-1} attributable to the symmetric and asymmetric stretches of carbonyl groups in an imide ring. The peaks at 1587 and 1187 cm^{-1} are assigned to the stretches of carbon-carbon double bond in benzene rings and ether linkages of APB, respectively (Figure 10). In the CP2-g-VGCNF sample, the absorption bands in their IR spectrum generally became broader than those of the free CP2-polyimide. However, most major peaks of CP2 are still identifiable in the region of 1000-2000 cm^{-1} , but there is practically no absorption detectable below 1000 cm^{-1} region. After free CP2 has been removed by THF washing, the resulting IR peaks become broader and the absorption intensity is generally lower than before.

On the other hand, the film of 5 wt% CP2/VGCNF blend exhibits essentially the same vibrational pattern as that of CP2 homopolymer. However, after CP2/VGCNF film has been suspended in THF for 2 days, the complete removal (extraction) of CP2 from the sample is confirmed by the spectrum of the black residue, which is devoid of the vibrational bands characteristic of CP2 in 750-2000 cm^{-1} region. (see Figure 11).

[Figure 10. IR spectra of (a) CP2 film, (b) 5wt% CP2-g-VGCNF film and (c) 5wt% CP2-g-VGCNF film after extraction with THF.]

[Figure 11. IR spectra of (a) CP2 film, (b) 5wt% CP2/VGCNF film and (c) 5wt% CP2-g-VGCNF powder after extraction with THF.]

Scanning Electron Microscope (SEM). High resolution SEM was used to evaluate the dispersion of the carbon nanofibers in CP2-polyimide matrix. The nanofibers of 0.1 wt% CP2-g-VGCNF are dispersed well in the polyimide matrix as shown in Figure 12a. Higher resolution SEM images demonstrate that the nanofibers were coated with the polymers and their diameters had increased roughly by 100-300 nm (Figure 12b). The CP2-g-VGCNF films containing 1

wt%, 2 wt% and 5% functionalized VGCNF also display relatively uniform dispersion (Figures 12c 12d and 12f). The good interfacial adhesion as manifested by continuity between CP2 and VGCNF is also observed (Figure 12e). However, the dispersion of the pristine VGCNF in CP2 is not as good as the functionalized VGCNF. The 2 wt% CP2/VGCNF film shows uniform dispersion in one area (Figure 13a) and large aggregates in other area (Figure 13b).

[Figure 12. SEM images of CP2-g-VGCNF (a) 0.1 wt% VGCNF ($\times 2k$), (b) 0.1 wt % VGCNF ($\times 20k$), (c) 1.0 wt% VGCNF ($\times 2k$), (d) 2.0 wt% VGCNF ($\times 2k$), (e) 2.0wt% VGCNF ($\times 300k$) and 5.0wt% VGCNF ($\times 2k$)]

[Figure 13. SEM images of CP2/VGCNF (a) 2.0 wt% VGCNF ($\times 2k$) and (b) 2.0 wt % VGCNF ($\times 2k$).]

Mechanical Properties. The nanocomposite films were cut into 50x5 mm slices and a Tinius Olsen tensometer was used to measure their tensile properties with a crosshead separation speed of 1 mm/min. As shown in Table 6, both the tensile strength and strain of CP2-g-VGCNF films increase as VGCNF content is increased from 0 to 5 wt%, indicating that the stiffness of nanocomposite films is directly increased with VGCNF content. The modulus increases from 3.3 to 4.8 GPa (a 45% increase) as the VGCNF contents increased from 0 to 5 wt% while the tensile strengths increase moderately. The cross sections of the thin films were examined with HR-SEM (Figure 14). Some nanofibers are broken under the stress, which indicates the good adhesion with the polymer matrix. Some simply are pulled out, leaving holes in the CP2 matrix and indicative of poor adhesion between the fibers and polymer matrix. On the other hand, the tensile strength, strain and modulus of CP2/VGCNF films are lower than the pristine CP2 film. The poor dispersion of the pristine VGCNF in CP2 together with the poor adhesion between them could be attributed to the lower mechanical properties of CP2/VGCNF films. The VGCNF aggregate as shown in Figure 13b can act as a defect instead of as a reinforcement. It is worth noting that in situ synthesis of MWNT-polyimide nanocomposites had led to improvement in mechanical properties in various degrees. For example, Jiang et al reported that the mechanical properties of the polyimide (Kapton)-based in situ nanocomposites were not improved significantly by the addition of pristine MWNTs; Young's modulus increased only 6% with 1.89

vol% of MWNT and decreased when MWNT content was further increased,²² whereas Ge *et al* claimed significant improvement for their MWNT-polyetherimide nanocomposites: 8-60% increase in tensile strength and 28-25% in modulus for MWNT content of 0.14-0.38 wt%.²³

[Table 6. Thin film tensile properties of CP2-g-VGCNF]

Table 7. Thin film tensile properties of CP2/VGCNF films

[Figure 14. SEM image of 0.1 wt% CP2-g-VGCNF after Instron testing]

Conclusion

In this work, we have shown that an amine-containing benzoic acid could be used to arylcarbonylate vapor grown carbon nanofibers and multi-walled carbon nanotubes via a Friedel-Crafts acylation reaction in an optimized PPA/P₂O₅ medium.²⁴ We believe this is the first example of carbon nanofibers that contain aromatic amines capable of further reactions under a conditions. The resulting H₂N-VGCNF (degree of functionalization ~ 5 atom%) was able to participate in the in situ polymerization of a dianhydride (6FDA) and a diamine (APB) to afford, after typical thermal curing, a series of polyimide-based nanocomposite (CP2-g-VGCNF) films, which contained 0.1 to 5 wt% of the functionalized VGCNF. Therefore, while our previous work has shown the feasibility of directly grafting the defect sites on either VGCNF via a Friedel-Crafts acylation reaction in poly(phosphoric acid) with a suitable, arylother-benzoic-acid type AB or AB₂ monomer in a one-pot fashion, this work further demonstrates the feasibility of in situ grafting of pre-functionalized VGCNF (most likely MWNT as well) with a rather common aromatic polyimide (CP2) under conventional AA+BB polymerization and thermal (solid-state) imidization conditions. In this two-stage preparation of in situ nanocomposites, the presence of pre-functionalized VGCNF has little or no adverse effect on the molecular weight of the resulting polyimide. However, based on the comparative results from solvent extraction experiments, there was more free polyimide present in nanocomposites described here than there were free poly(ether-ketone)s in the previous cases.^{6b,e,f} This may be arisen from the kinetics of polymerization. Last but not least, we confirm that the functionalized VGCNF has better dispersion and stronger bonding with the matrix polymer in the CP2 films than its pristine counterpart, as evidenced by the better mechanical properties and the comparative SEM data.

The electrical response of these nanocomposite films has also been investigated for use as high temperature electrostatic dissipation (ESD) and electromagnetic interference (EMI) shielding films and as thermal electric switches. The details of the results and discussion will be presented elsewhere.²⁵

Acknowledgement. Gary Price and Marlene Houtz (University of Dayton Research Institute) for SEM images and TGA data, respectively. This project was supported by funding from Wright Brother Institute (Dayton), Office of Scientific Research (AFOSR) and Materials & Manufacturing Directorate, US Air Force Research Laboratory.

List of Tables

Table 1. Element analysis data for pristine and functionalized VGCNF.

Table 2. Molecular weights and molecular distributions of CP2-g-VGCNF

Table 3. Molecular weights and molecular distributions of CP2/VGCNF films

Table 4. Physical properties of CP2-g-VGCNF films

Table 5. Thermal properties of CP2/VGCNF films

Table 6. Thin film tensile properties of CP2-g-VGCNF

Table 7. Thin film tensile properties of CP2/VGCNF films

List of Schemes

Scheme 1. Functionalization of VGCNF with 3-aminophenoxy-4-benzoic acid (i) NMP, K_2CO_3 , 160 °C, 6 h. (ii) PPA, H_2O , 120 °C, 8 h. (iii) P_2O_5 /PPA, 130 °C, 3 d.

Scheme 2. PPA-treated VGCNF (i) P_2O_5 /PPA, 130 °C, 3 d.

Scheme 3. Synthesis of CP2-g-VGCNF nanocomposites via in situ polymerization of 6FDA (**7**), APB (**8**) and H_2N -g-VGCNF (**6**). (i). DMAc, room temperature. (ii). 100 °C, 24h; 150 °C, 4h; 200 °C, 2h; 250 °C, 1h.

Scheme 4. Synthesis of VGCNF/CP2 blends via in situ polymerization of 6FDA (**7**), APB (**8**) and pristine VGCNF (**5**). (i). DMAc, room temperature, 24h. (ii). 100 °C, 24h; 150 °C, 4h; 200 °C, 2h; 250 °C, 1h.

List of Figures

Figure 1. FT-IR spectra of (a) pristine VGCNF, (b) PT-VGCNF, (c) 3-aminophenoxy-4-benzoic acid (**4**) and (d) NH₂-VGCNF (**6**).

Figure 2. SEM images of (a) as-received VGCNF ($\times 100k$) and (b) NH₂-VGCNF ($\times 70k$).

Figure 3. TGA thermograms with heating rate of 10 °C/min of pristine VGCNF and H₂N-VGCNF

Figure 4. SEM images of (a) as-received VGCNF ($\times 25k$) and (b) PT-VGCNF ($\times 25k$).

Figure 5. CP2 films containing VGCNF

Figure 6. CP2 film during THF extraction (a) 5wt% CP2-g-VGCNF and (b) 5wt% CP2/VGCNF blend.

Figure 7. CP2 film after THF extraction (a) 5wt% CP2-g-VGCNF and (b) 5wt% CP2/VGCNF blend.

Figure 8. DSC thermograms of (a) CP2-g-VGCNF samples and (b) CP2/VGCNF blends with heating rate of 10 °C/min

Figure 9. TGA thermograms of CP2-g-VGCNF with heating rate of 10 °C/min (a) in air and (b) in helium

Figure 10. IR spectra of (a) CP2 film, (b) 5wt% CP2-g-VGCNF film and (c) 5wt% CP2-g-VGCNF film after extraction with THF.

Figure 11. IR spectra of (a) CP2 film, (b) 5wt% CP2/VGCNF film and (c) 5wt% CP2-g-VGCNF powder after extraction with THF.

Figure 12. SEM images of CP2-g-VGCNF (a) 0.1 wt% VGCNF ($\times 2k$), (b) 0.1 wt % VGCNF ($\times 20k$), (c) 1.0 wt% VGCNF ($\times 2k$), (d) 2.0 wt% VGCNF ($\times 2k$), (e) 2.0wt% VGCNF ($\times 300k$) and 5.0wt% VGCNF ($\times 2k$)

Figure 13. SEM images of CP2/VGCNF (a) 2.0 wt% VGCNF ($\times 2k$) and (b) 2.0 wt % VGCNF ($\times 2k$).

Figure 14. SEM image of 0.1 wt% CP2-g-VGCNF after Instron testing

Table 1. Elemental analysis data for pristine and functionalized VGCNF.

Sample	Elemental Analysis	C (%)	H (%)	N (%)	O (%)
Pristine	Calcd	100	0	0	0
VGCNF	Found	99.02	1.01	<0.20 ^a	<0.10 ^a
H ₂ N-	Calcd ^b	87.60	2.23	3.10	7.07
VGCNF	Found	87.11	2.33	3.43	6.40
PT-	Calcd	100	0	0	0
VGCNF	Found	98.66	0.93	<0.20 ^a	<0.10 ^a

^a Less than detection limit.

^b Its molecular formula of C₁₆₅H₅₀N₅O₁₀ is based on the assumption that for every 100 carbon there are 5 4-(3-aminophenoxy)benzoyl groups attached according to TGA (air) result. The molecular formula of 4-(3-aminophenoxy)benzoyl group are C₁₃H₁₀NO₂. The calculation is based on the following equation:

$$\text{Theoretical Weight Loss at } 700\text{ }^{\circ}\text{C} = \frac{n \times \text{MW}_{\text{amine}}}{100 \times \text{MW}_c + n \times \text{MW}_{\text{amine}}} \times 100$$

Where n is the number of 4-(3-aminophenoxy)benzoyl groups attached to VGCNF every 100 carbon. MW_{amine} is the molecular weight of 4-(3-aminophenoxy)benzoyl group, which is 212.22. MW_c is the molecular weight of carbon, which is 12.01.

When n is equal to 5, Theoretical Weight Loss at 700 °C is 46.9% based on above equation. This value is in good agreement with the weight loss at 700 °C (45.6%).

Table 2. Molecular weights and molecular distributions of CP2-g-VGCNF

VGCNF Content (wt%)	M _n ^a	M _w ^a	PDI ^a	Insoluble Content in THF (wt%)	Content of CP2 grafted onto VGCNF (wt%) ^b	MW/chain ^c	DP/chain ^d
0	84,200	238,400	2.83	0	0	-	-
0.1	126,200	371,300	2.94	2.3	2.2	5,280	15.1
0.3	91,400	238,600	2.61	6.1	5.8	4,640	13.2
1.0	55,600	146,200	2.63	15.4	14.4	3,460	9.88
2.0	56,780	135,700	2.39	30.9	28.9	3,470	9.91
5.0	41,900	94,300	2.25	52.5	47.5	2,280	6.51

^a Molecular weights and MW distributions of CP2 soluble in THF measured by size-exclusion liquid chromatography in THF.

^b Weight percentage of CP2 grafted onto VGCNF. It is equal to insoluble content in THF minus VGCNF content.

^c Molecular weights of CP2 insoluble in THF calculated by the following equation:

Content of CP2 grafted onto VGCNF

$$\text{MW/chain} = \frac{\text{Content of CP2 grafted onto VGCNF}}{(\text{VGCNF Content} / 12) * 0.05}$$

Where 0.05 is reactive sites on H₂N-g-VGCNF (5 atom%). 12 is carbon formula weight.

^d Degree of polymerization (DP)/chain = (MW/chain)/350.3 (FW of repeat unit: C_{19.5}H₄F₃NO₃).

Table 3. Molecular weights and molecular distributions of CP2/VGCNF films

VGCNF (wt%)	M_n^a	M_w^a	PDI ^a	Insoluble Content in THF (wt%)
0	84,200	238,400	2.83	0
0.1	126,200	415,600	3.29	0.10
0.3	85,200	198,000	2.33	0.33
1.0	62,060	154,100	2.63	1.06
2.0	70,530	153,700	2.18	1.88
5.0	57,090	128,460	2.25	5.32

^a Molecular weights and molecular distributions (PDI) of CP2 soluble in THF measured by size-exclusion liquid chromatography in THF.

Table 4. Physical properties of CP2-g-VGCNF films

		DSC	TGA			
			in helium		in air	
VGCNF (wt%)	$[\eta]^a$ (dL/g)	T_g^b (°C)	$T_{d5\%}^c$ (°C)	Char ^d (%)	$T_{d5\%}^c$ (°C)	Char ^d (%)
0	0.42	199	530	56.5	526	1.14
0.1	0.65	201	528	52.9	526	0.33
0.3	0.94	202	531	55.7	520	0.38
1.0	1.12	199	529	56.4	525	0.55
2.0	1.37	197	525	56.5	520	0.51
5.0	1.43	196	526	53.6	520	1.26

^a Intrinsic viscosity measured in NMP at 30.0±0.1°C.

^b Inflection in baseline on DSC thermogram obtained in N₂ with a heating rate of 10 °C/min.

^c Temperature at which 5% weight loss occurred on TGA thermogram obtained with a heating rate of 10 °C/min.

^d Char yield at 850 °C.

Table 5. Thermal properties of CP2/VGCNF films

VGCNF (wt%)	DSC	TGA			
	T_g^a (°C)	in helium		in air	
		$T_{5\%}^c$ (°C)	Char ^d (%)	$T_{5\%}^c$ (°C)	Char (%)
0	199	524	53.5	521	0.15
0.1	203	531	54.6	522	0.00
0.3	202	530	56.1	520	0.22
1.0	200	532	55.3	518	0.11
2.0	195	527	57.2	521	0.23
5.0	194	528	56.4	521	0.11

^a Inflection in baseline on DSC thermogram obtained in N₂ with a heating rate of 10 °C/min.

^b Temperature at which 5% weight loss occurred on TGA thermogram obtained with a heating rate of 10 °C/min.

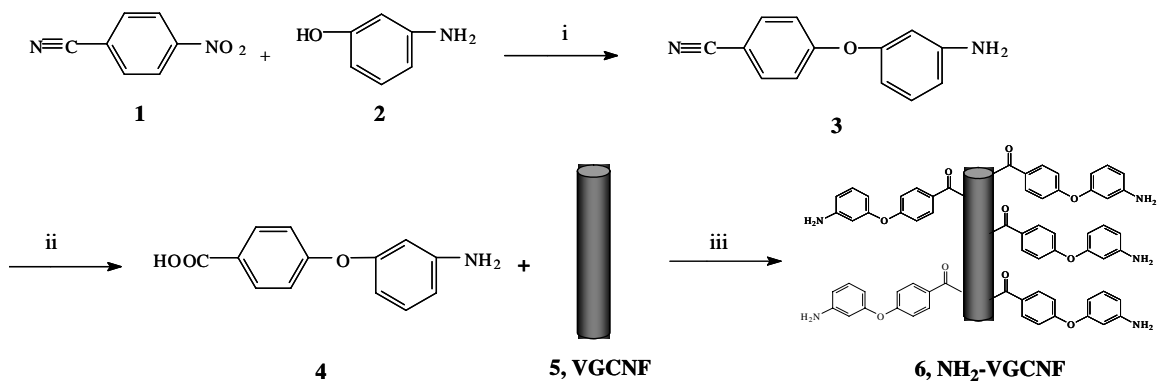
^d Char yield at 850 °C.

Table 6. Thin film tensile properties of CP2-g-VGCNF

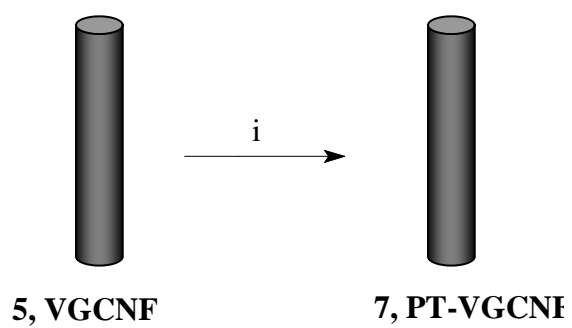
VGCNF (wt%)	Tensile Strength (MPa)	Tensile Modulus (GPa)	Tensile Strain (%)
0	116±5	3.3±0.2	6.3±1.1
0.1	120±11	3.5±0.1	6.2±0.5
0.3	126±11	3.6±0.2	6.4±0.7
1.0	131±7	3.5±0.2	6.2±1.2
2.0	122±5	3.7±0.2	4.7±0.6
5.0	124±5	4.8±0.4	5.9±0.8

Table 7. Thin film tensile properties of CP2/VGCNF films

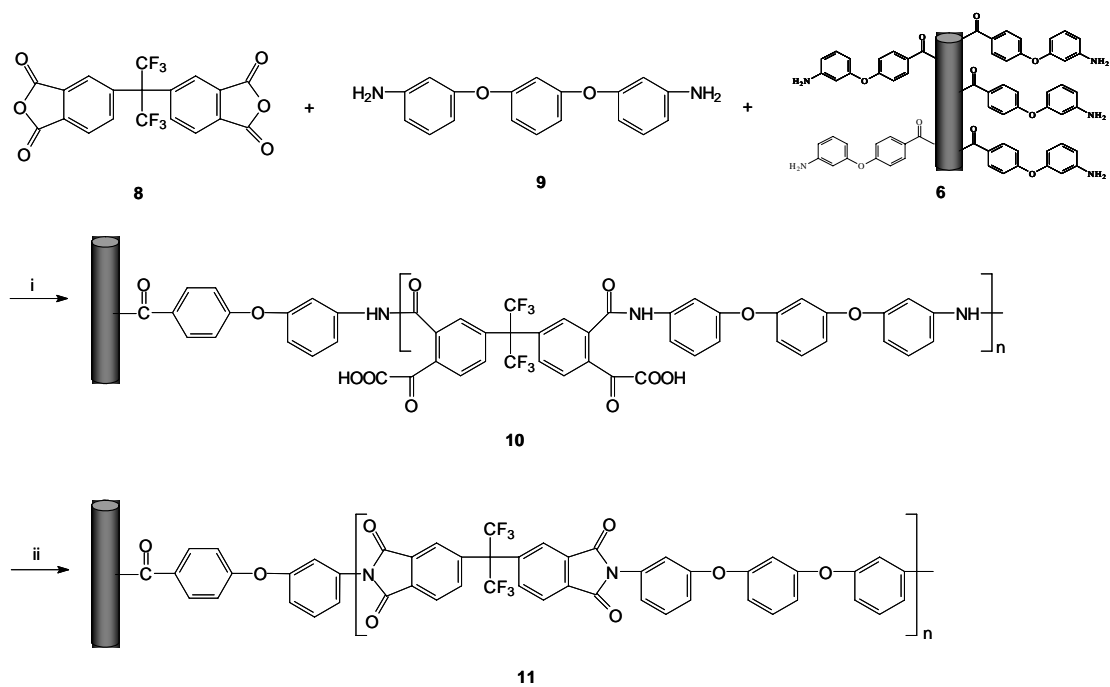
VGCNF (wt%)	Tensile Strength (MPa)	Tensile Modulus (GPa)	Tensile Strain (%)
0	116±5	3.3±0.2	6.3±1.1
0.1	84.4±10.8	2.9±0.2	5.1±0.3
0.3	102±13	3.1±0.4	4.6±0.3
1.0	96.5±13.1	3.2±0.3	5.0±0.5
2.0	87.5±11.4	3.0±0.2	4.2±0.6
5.0	52.1±6.4	2.6±0.3	2.3±0.2



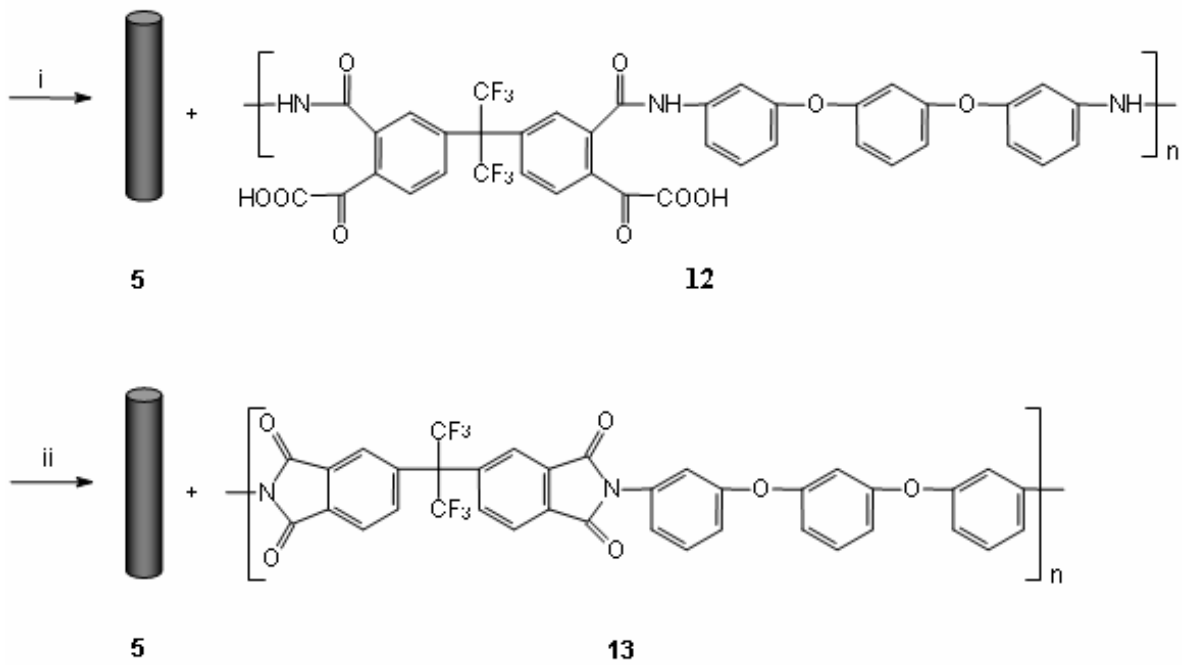
Scheme 1. Functionalization of VGCNF with 3-aminophenoxy-4-benzoic acid (i) NMP, K_2CO_3 , 160 °C, 6 h. (ii) PPA, H_2O , 120 °C, 8 h. (iii) P_2O_5 /PPA, 130 °C, 3 d.



Scheme 2. PPA-treated VGCNF (i) $\text{P}_2\text{O}_5/\text{PPA}$, 130 °C, 3 d.



Scheme 3. Synthesis of CP2-g-VGCNF nanocomposites via in situ polymerization of 6FDA (7), APB (8) and H₂N-g-VGCNF (6). (i). DMAc, room temperature. (ii). 100 °C, 24h; 150 °C, 4h; 200 °C, 2h; 250 °C, 1h.



Scheme 4. Synthesis of VGCNF/CP2 blends via in situ polymerization of 6FDA (**7**), APB (**8**) and pristine VGCNF (**5**). (i). DMAc, room temperature, 24h. (ii). 100 °C, 24h; 150 °C, 4h; 200 °C, 2h; 250 °C, 1h.

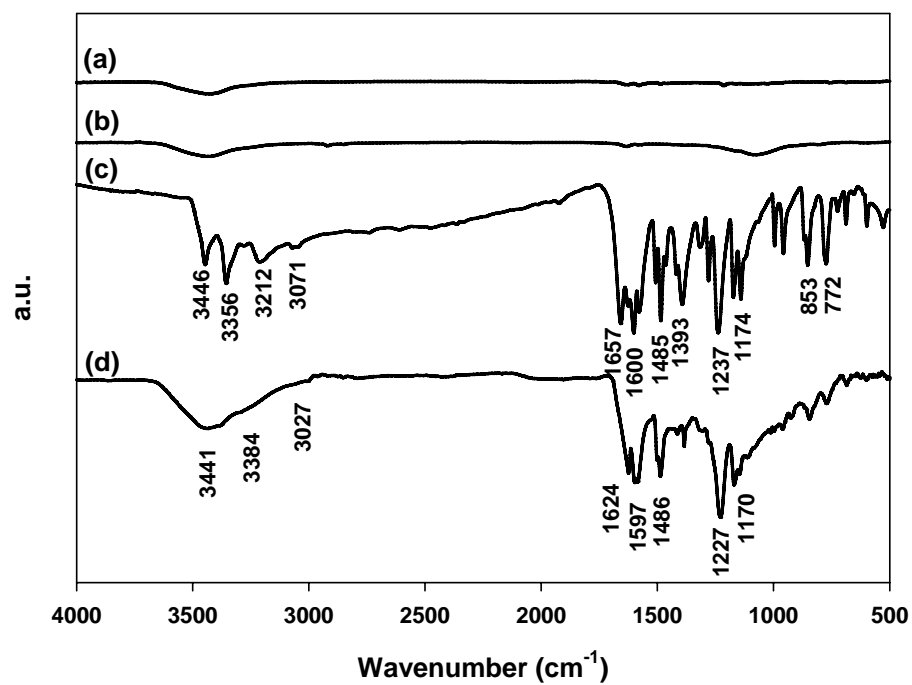


Figure 1. FT-IR spectra of (a) pristine VGCNF, (b) PT-VGCNF, (c) 3-aminophenoxy-4-benzoic acid (**4**) and (d) NH₂-VGCNF (**6**).

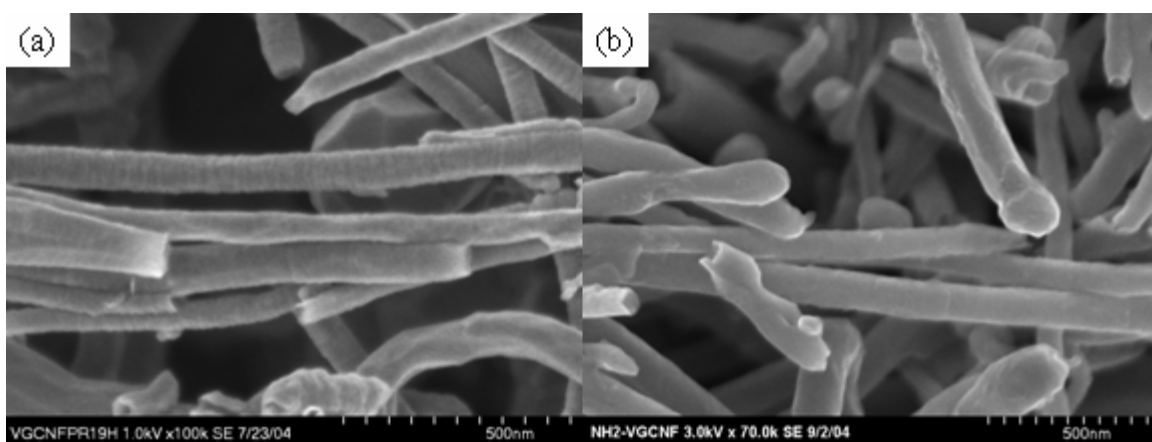


Figure 2. SEM images of (a) as-received VGCNF ($\times 100k$) and (b) NH_2 -VGCNF ($\times 70k$).

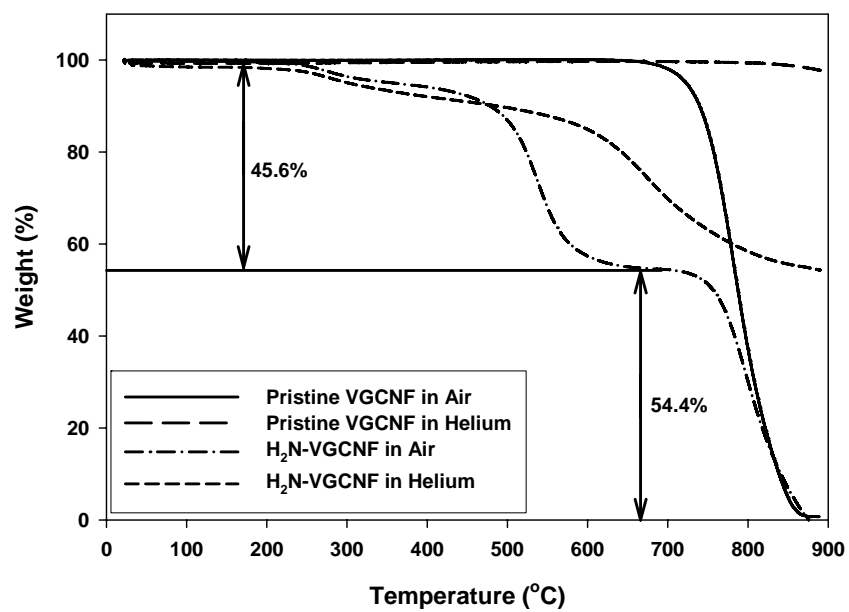


Figure 3. TGA thermograms with heating rate of 10 °C/min of pristine VGCNF and H₂N-VGCNF

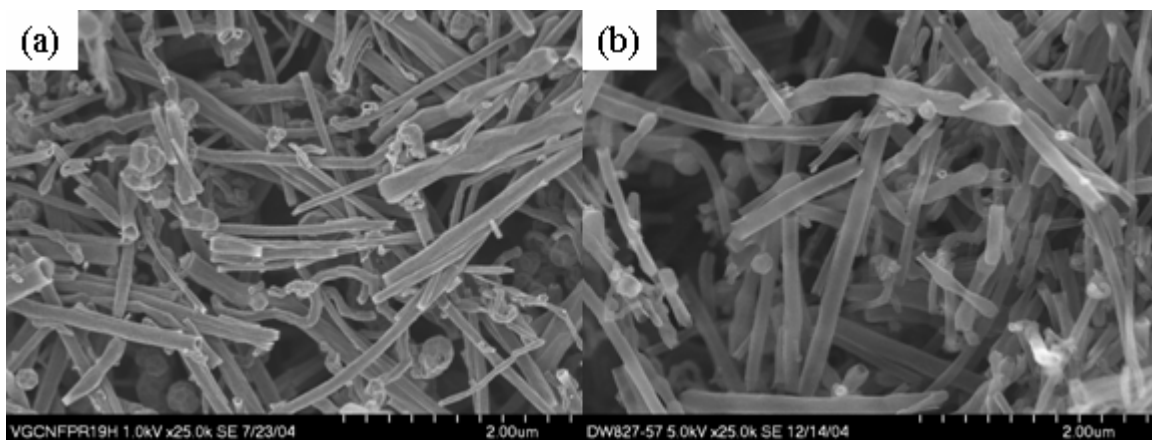


Figure 4. SEM images of (a) as-received VGCNF ($\times 25k$) and (b) PT-VGCNF ($\times 25k$).

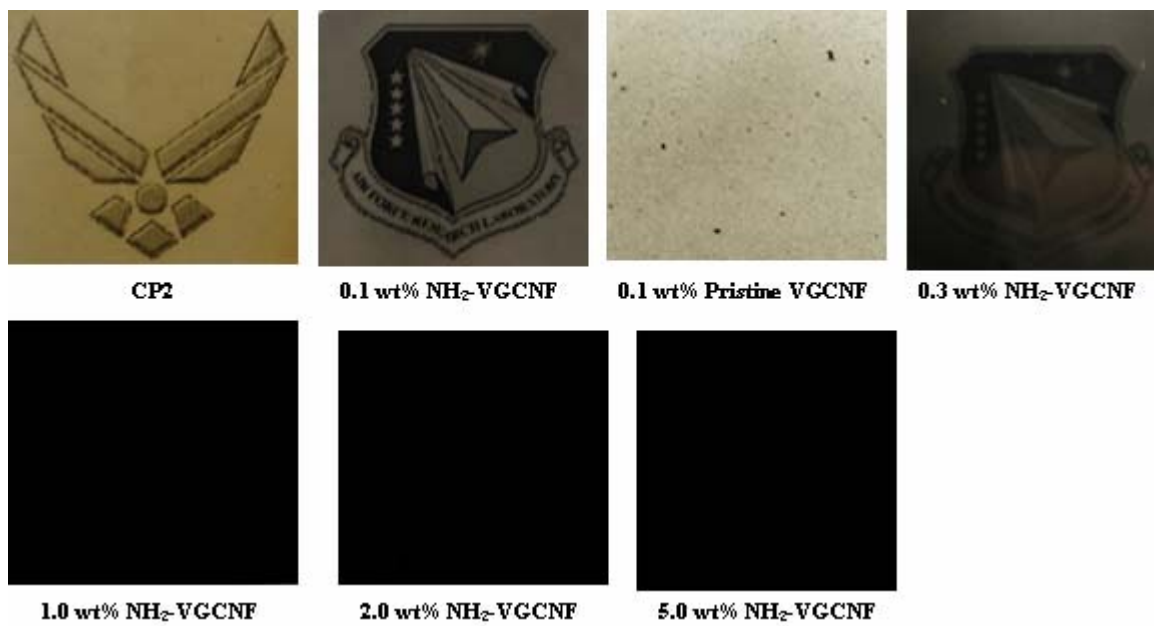


Figure 5. CP2 films containing VGCNF

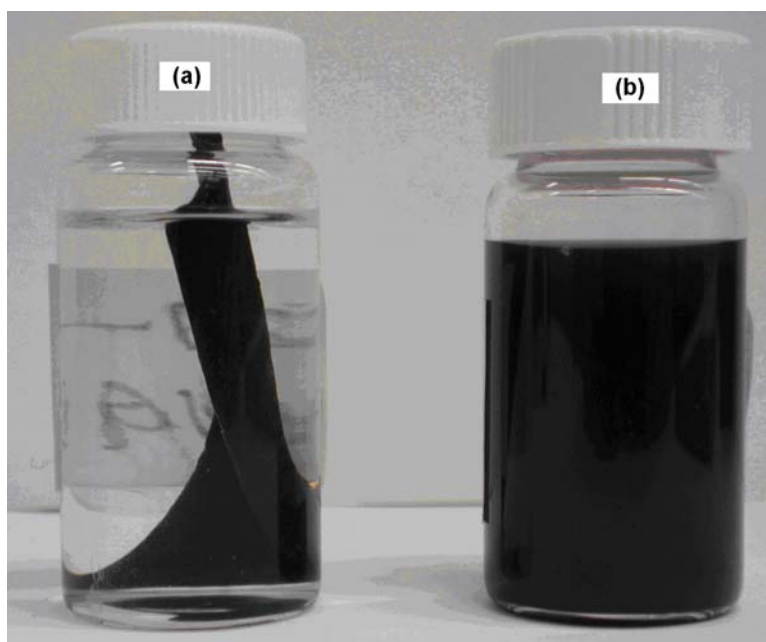


Figure 6. CP2 film during THF extraction (a) 5wt% CP2-g-VGCNF and (b) 5wt% CP2/VGCNF blend.

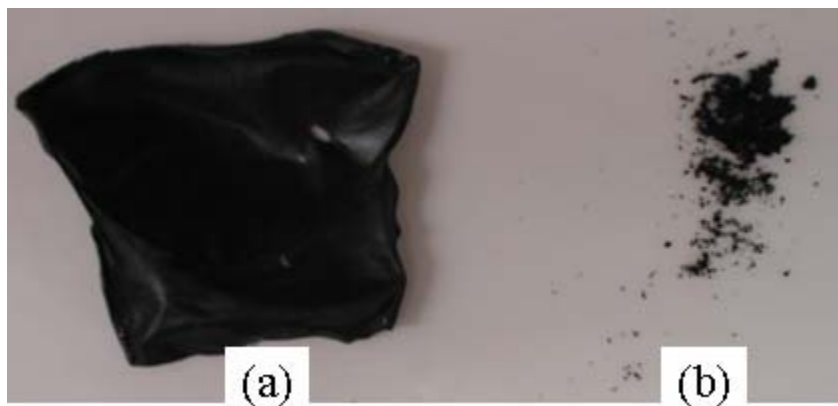


Figure 7. CP2 film after THF extraction (a) 5wt% CP2-g-VGCNF and (b) 5wt% CP2/VGCNF blend.

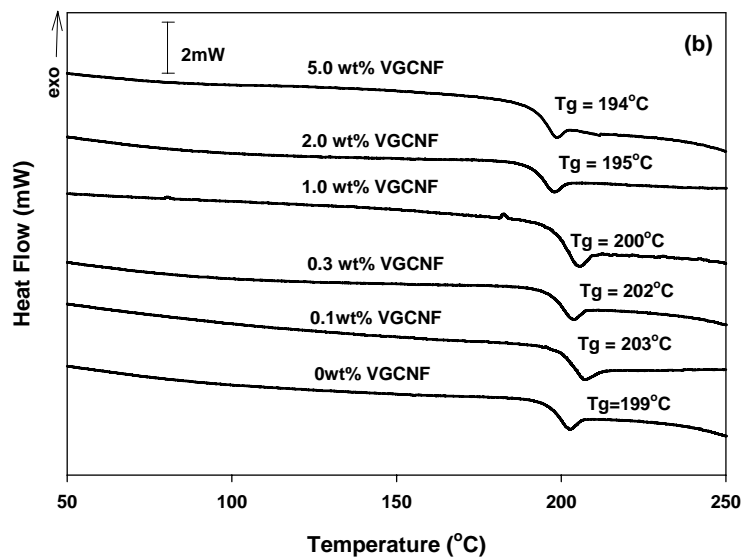
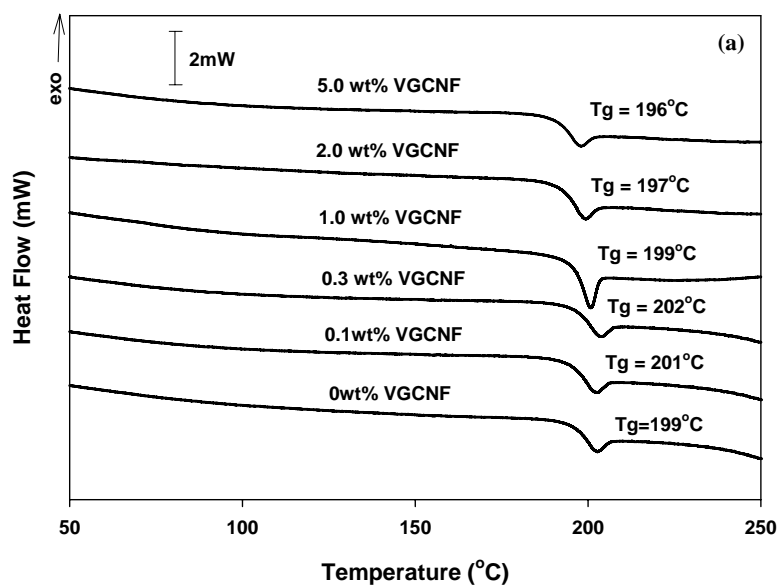


Figure 8. DSC thermograms of (a) CP2-g-VGCNF samples and (b) CP2/VGCNF blends with heating rate of 10 °C/min

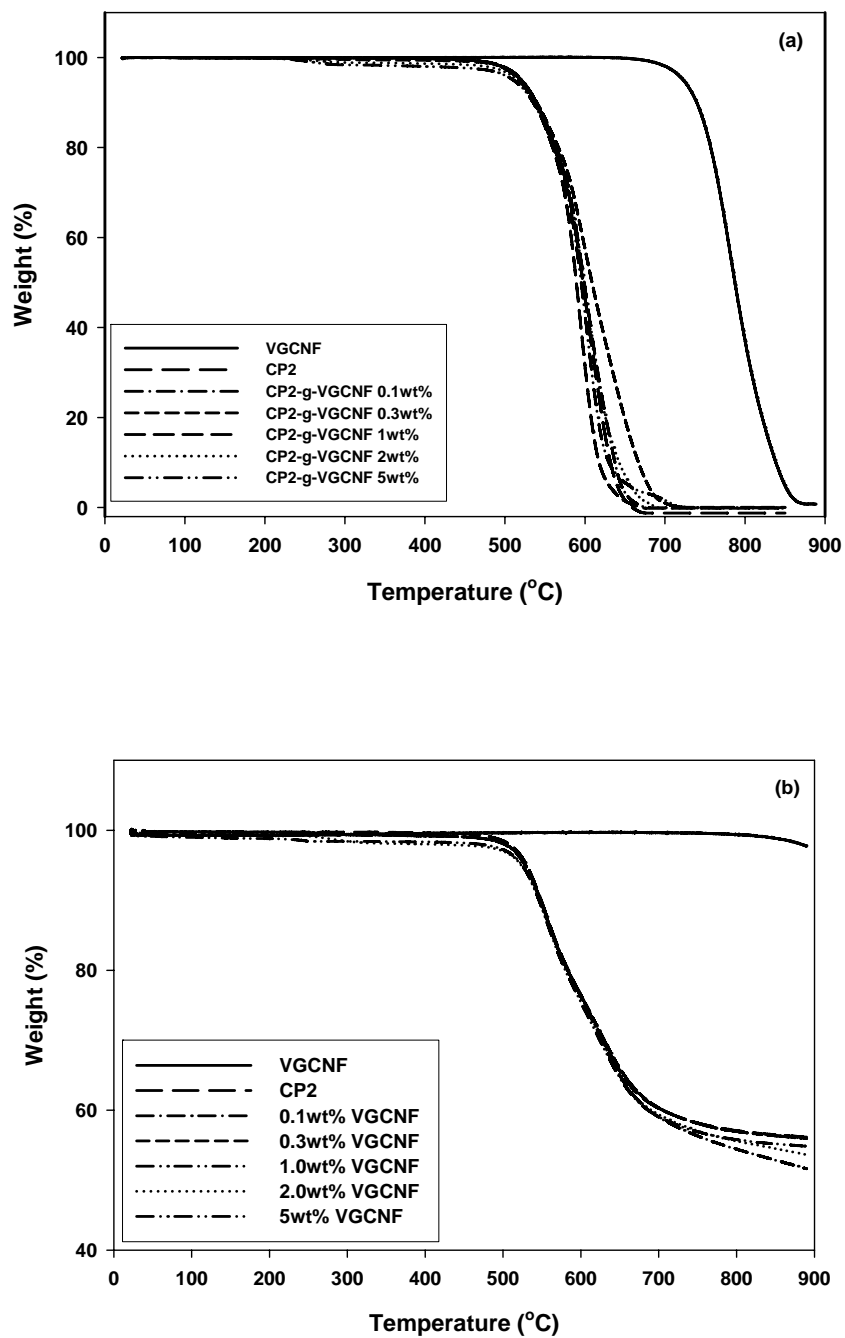


Figure 9. TGA thermograms of CP2-g-VGCNF with heating rate of 10 °C/min (a) in air and (b) in helium

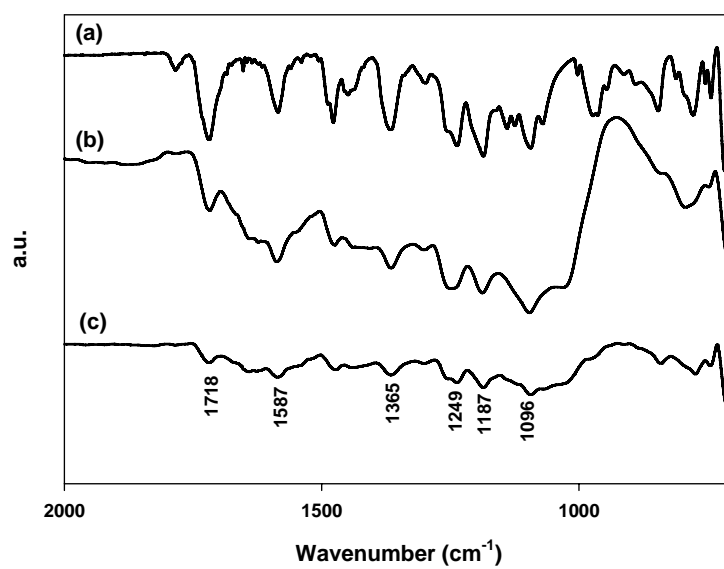


Figure 10. IR spectra of (a) CP2 film, (b) 5wt% CP2-g-VGCNF film and (c) 5wt% CP2-g-VGCNF film after being extracted with THF.

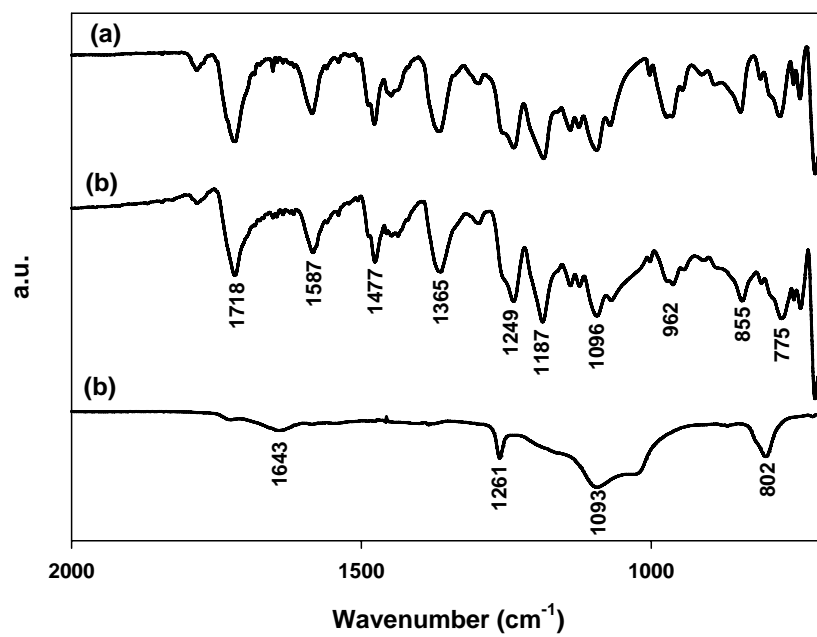


Figure 11. IR spectra of (a) CP2 film, (b) 5 wt% CP2/VGCNF film and (c) 5wt% CP2-g-VGCNF powder after being extracted with THF.

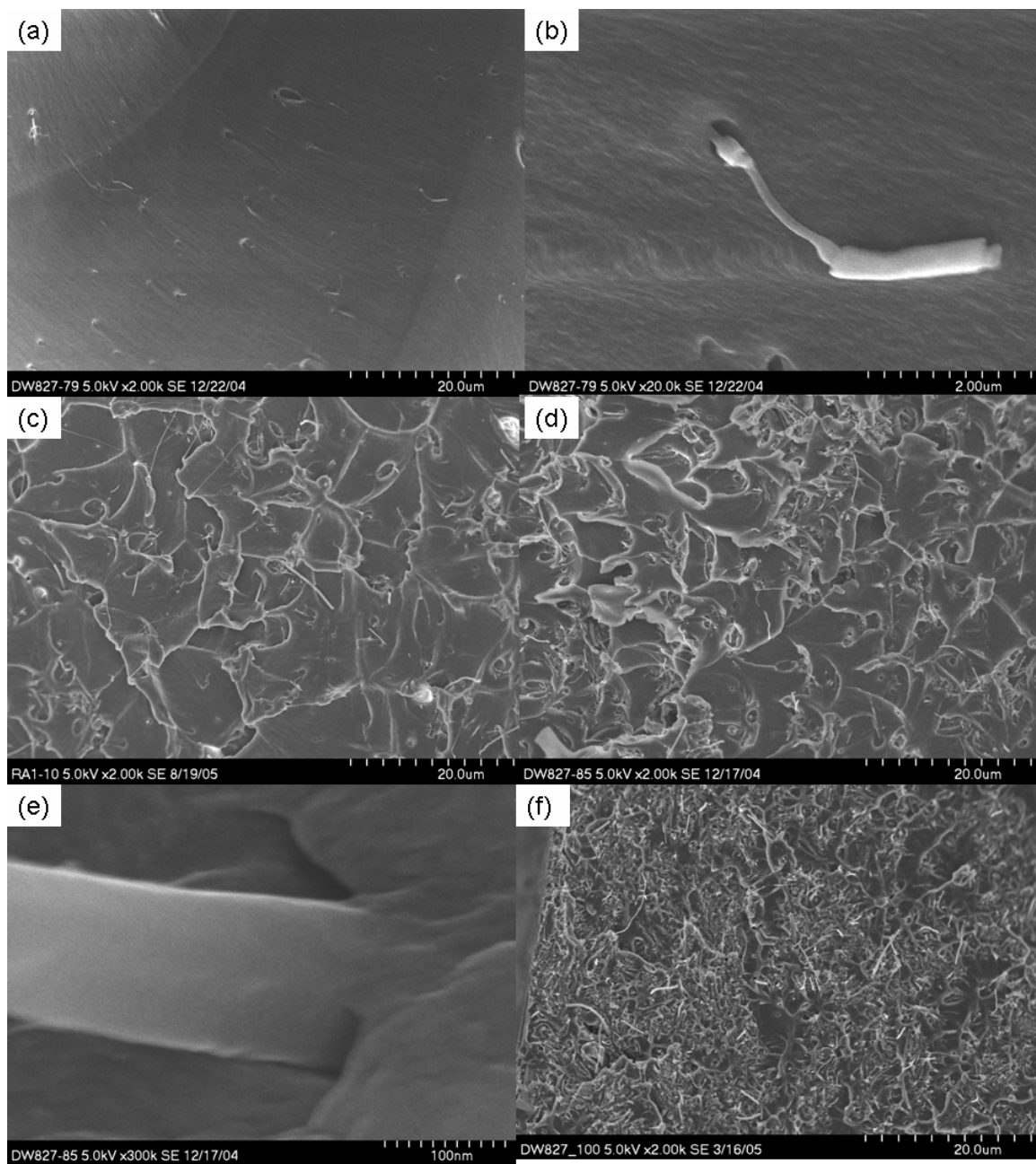


Figure 12. SEM images of CP2-g-VGCNF (a) 0.1 wt% VGCNF ($\times 2k$), (b) 0.1 wt % VGCNF ($\times 20k$), (c) 1.0 wt% VGCNF ($\times 2k$), (d) 2.0 wt% VGCNF ($\times 2k$), (e) 2.0wt% VGCNF ($\times 300k$) and 5.0wt% VGCNF ($\times 2k$)

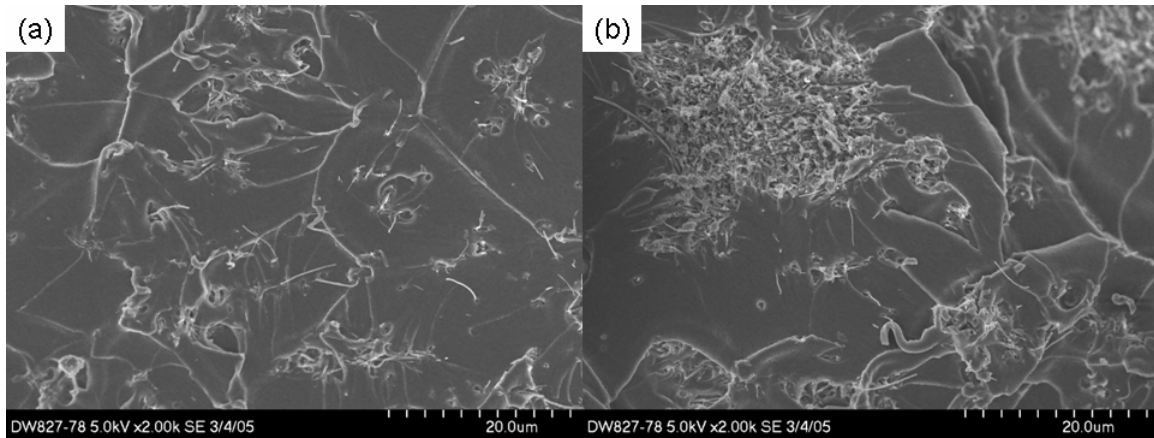


Figure 13. SEM images of CP2/VGCNF (a) 2.0 wt% VGCNF ($\times 2k$) and (b) 2.0 wt % VGCNF ($\times 2k$).

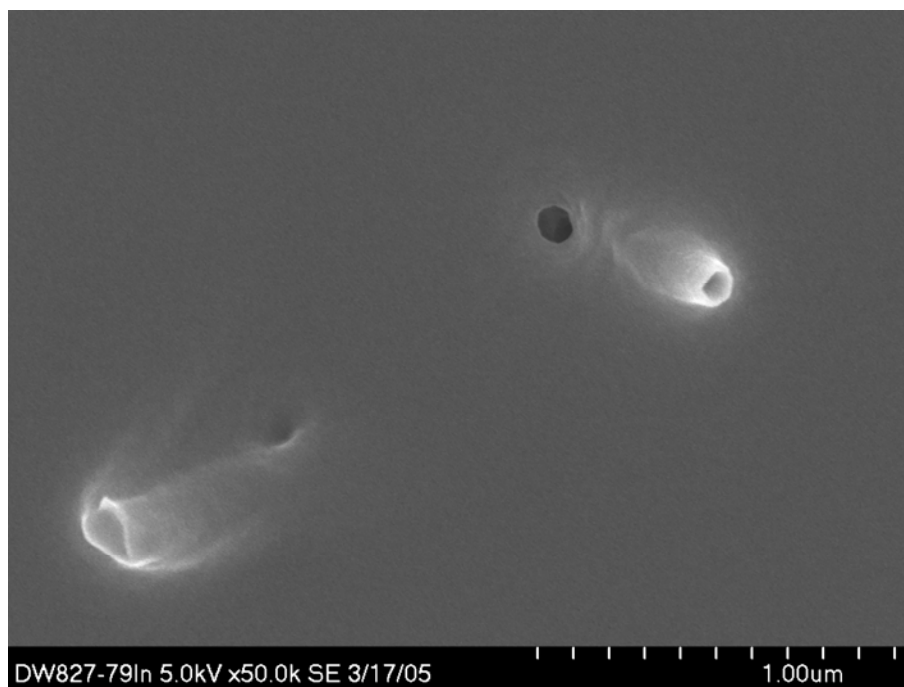


Figure 14. SEM image of 0.1 wt% CP2-g-VGCNF after Instron testing ($\times 50K$)

References

- ¹ Maruyama, B.; Alam, K. *SAMPE Journal* **2002**, 38, (3), 59-70.
- ² Dimitrios Tasis, Nikos Tagmatarchis, Alberto Bianco, and Maurizio Prato., “Chemistry of Carbon Nanotubes” *Chem. Rev.* **2006**, 106, 1105-1136|
- ³ Chen, J.; Hamon, M.A.; Hu, H.; Chen, Y.; Rao, A. M.; Eklund, P.C. and Haddon, R. C. *Science* 1998, **282**, 95.
- ⁴ Bahr, J. L.; Mickelson, E. T.; Bronikowski, M.J.; Smalley, R. E. and Tour, J. M. *Chem. Commun.* 2001, **3**, 193.
- ⁵ Dyke, C. A. and Tour J.M. *J. Am. Chem. Soc.* 2003, **125**, 1156.
- ⁶ (a) Baek, J.-B.; Lyons, C. B.; Tan, L.-S. *J. Mater. Chem.* **2004**, 14, 2052. (b) Baek, J.-B.; Lyons, C. B.; Tan, L.-S. *Macromolecules* **2004**, 37, 8278. (c) Baek, J.-B.; Park, S. Y.; Price, G.E.; Lyons, C. B.; Tan, L. S. *Polymer* **2004**, 46, 1543. (d) Lee, H.-J.; Oh, S.-J.; Choi, J.-Y.; Kim, J. W.; Han, J.; Tan, L.-S.; Baek, J.-B. *Chem. Mater.* **2005**, 17, 5057-5064. (e) Oh, S.-J.; Lee, H.-J.; Keum, D.-K.; Lee, S.-W.; Wang, D. H.; Park, S.-Y.; Tan, L.-S.; Baek, J.-B. *Polymer* **2006**, 47, 1132-1140. (f) Wang, D.H.; Baek, J.-B.; Tan, L.-S. *Mater. Sci. Eng. B.* **2006**, 132, 103.
- ⁷ (a) Wei, G.; Fujiki, K.; Saitoh, H.; Shirai, K.; Tsubokawa, N. *Polymer J. (Tokyo, Japan)* **2004**, 36, (4), 316-322; (b) Wei, G.; Saitoh, S.; Saitoh, H.; Fujiki, K.; Yamauchi, T.; Tsubokawa, N. *Polymer* **2004**, 45, (26), 8723-8730; (c) Wei, G.; Shirai, K.; Fujiki, K.; Saitoh, H.; Yamauchi, T.; Tsubokawa, N. *Carbon* **2004**, 42, (10), 1923-1929.
- ⁸ (a) Wilson, D.; Stenzenberger, H. D.; Hergenrother, P. M. *Polyimides*, Chapman and Hall: New York, **1990**, pp. 1-78. (b) Hergenrother, P. M. *Recl. Trav. Chim. Pays-Bas.* **1991**, 110, 481. (c) Hergenrother, P. M. In *Polyimides and Other High-Temperature Polymers*; Abadie, M. J. M.; Sillion, B. Ed.; Elsevier: New York, **1991**, pp. 1-18. (d) Critchley, J. P.; Knight, G. J.; Wright, W. W. *Heat Resistant Polymers*; Plenum Press: New York, **1983**, pp. 186-258. (e) Sroog, C. E. *J. Polym. Sci., Macromol. Rev.* **1976**, 11,

161. (f) Cheng, S. Z. D.; Li, F.; Savitski, E. P.; Harris, F. W. *Trends in Polym. Sci.* **1997**, 5, 51.

⁹ (a) Yu, A.; Hu, H.; Bekyarova, E.; Itkis, M. E.; Gao, J.; Zhao, B.; Haddon, R. C. *Compos. Sci. Tech.* **2006**, 66, (9), 1190-1197. (b) Delozier, D. M.; Tigelaar, D. M.; Watson, K. A.; Smith, J. G.; Klein, D. J.; Lillehei, P. T.; Connell, J. W. *Polymer* **2005**, 46, (8), 2506-2521; (c) Delozier, D. M.; Watson, K. A.; Smith, J. G.; Connell, J. W. *Compos. Sci. Tech.* **2005**, 65, (5), 749-755; (d) Styers-Barnett, D. J.; Ellison, S. P.; Park, C.; Wise, K. E.; Papanikolas, J. M. *J. Phys. Chem. A* **2005**, 109, (2), 289-292. (e) Grujicic, M.; Cao, G.; Roy, W. N. *J. Mater. Sci.* **2004**, 39, (14), 4441-4449; (f) Delozier, D. M.; Tigelaar, D. M.; Watson, K. A.; Smith, J. G., Jr.; Lillehei, P. T.; Connell, J. W. *Internat. SAMPE Symp. Exhib.* **2004**, 49, (SAMPE 2004), 2139-2151; (g) Qu, L.; Lin, Y.; Hill, D. E.; Zhou, B.; Wang, W.; Sun, X.; Kitaygorodskiy, A.; Suarez, M.; Connell, J. W.; Allard, L. F.; Sun, Y.-P. *Macromolecules* **2004**, 37, (16), 6055-6060. (h) Odegard, G. M.; Gates, T. S.; Wise, K. E.; Park, C.; Siochi, E. J. *Compos. Sci. Tech.* **2003**, 63, (11), 1671-1687; (i) Smith, J. G., Jr.; Watson, K. A.; Thompson, C. M.; Connell, J. W. *Internat. SAMPE Tech. Conf.* **2002**, 34, 365-376.

¹⁰ Carneiro, O. S.; Covas, J. A.; Bernardo, C. A.; Caldeira, G.; Hattum, F. W. J. V.; Ting, J. M.; Alig, R. L.; Lake, M. L. *Compos. Sci. Technol.* **1998**, 58, 401-407.

¹¹ Singh, C.; Quested, T.; Boothroyd, C. B.; Thomas, P.; Kinloch, I. A.; Abou-Kandil, A. I.; Windle, A. H. *J. Phys. Chem. B* **2002**, 106, 10915-10922.

¹² CHRISKEV Company, Inc., 5109 W. 111th Terrace, Leawood, KS 66211-1742.

¹³ (A) Schramm, J.; Radlmann, E.; Lohwasser, H.; Nischk, G. *Justus Liebigs Annalen der Chemie* **1970**, 740, 169; (b) Dann, O. Fick, H.; Pietzner, B.; Walkenhorst, E.; Fernbach, R.; Zeh, D. *Justus Liebigs Annalen der Chemie* **1975**, 1, 160; (c) Benson, D.A.; Karsch-Mizrachi, I.; Lipman, D.J.; Ostell, J.; Rapp, B.A.; Wheeler, D.L. *Genbank. Nucl. Acids Res.* **2000**, 28,15.

¹⁴ Irwin, R.S. *US Patent 5,395,917*, **1995**.

¹⁵ Baek, J.-B.; Tan, L.-S. *Polymer* **2003**, *44*, 4135.

¹⁶ (a) Li, J.; Vergne, M.J.; Mowles, E.D.; Zhong, W.-H.; Hercules, D.M.; Lukehart, C.M. *Carbon* **2005**, *43*, 2883; (b) Baker, S.E.; Tse, K.-Y.; Hindin, E.; Nichols, B.M.; Clare, T.L.; Hamers, Robert J. *Chem. Mater.* **2005**, *17*, 4971; (c) Saeed, K.; Park, S.-Y.; Lee, H.-J.; Baek, J.-B.; Huh, W.-S. *Polymer* **2006**, *47*, 8019; (d) Wang, Y.; Iqbal, Z.; Malhotra, S.V. *Chem. Phys. Lett.* **2005**, *402*, 96.

¹⁷ (a) Volksen, W.; Cotts, P.M. in *Polyimides, Vol. I* (ed. K.L. Mittal), Plenum Press **1984**, p163; (b) Walker, C.C. *J. Polym. Sci. PartA: Polym. Chem.* **1985**, *30*, 3037.

¹⁸ (a) Curran, S.; Ajayan, P.M.; Blau, W.; Carroll, D.L.; Coleman, J.N.; Dalton, A.B.; Davey, A.P.; Drury, A.; McCarthy, B.; Strevens, A. *Adv. Maert.* **1998**, *10*, 1091; (b) Chen, R.J.; Zhang, Y.; Wang, D.; Dai, H. *J. Am. Chem. Soc.* **2001**, *123*, 3838.

¹⁹ (a) Ueberreiter, K.; Kanig, G. *J. Colloid Sci.* **1952**, *7*, 569; (b) Fox, T. G. *Bull. Amer. Phys. Soc.* **1956**, *1*, 123; (c) Cohen, M. H., Turnbull, D. *J. Chem. Phys.* **1959**, *31*, 1164.

²⁰ Watson, K. A.; Smith, J. G.; Connell, J. W. *Internat. SAMPE Tech. Conf.* **2001**, *33*, 1551-1560.

²¹ (a) Becker, O.; Cheng, Y.-B.; Valey, R.J.; Simon, G.P. *Macromolecules* **2003**, *36*, 1616; (b) Yu, D. H.; Wang, B.; Feng, Y.; Fang, Z. P. *J. Appl. Polym Sci.* **2006**, *102*, 1509.

²² X. Jiang, Y. Bin, M, Matsou *Polymer* **2005**, *46*, 7418-7424.

²³ Ge, J. J.; Zhang, D.; Li, Q.; Hou, H.; Graham, M. J.; Dai, L.; Harris, F.; Cheng, S. Z. D. *J. Am. Chem. Soc.* **2005**, *127*, 9984-9985.

²⁴ We have confirmed that this method is also applicable to MWNT; results to be published.

²⁵ Arlen, M. J.; Wang, D. H.; Tan, L.-S.; Vaia, R. A. to be submitted.